Photochemical & Photobiological Sciences (2022) 21:397–419
https://doi.org/10.1007/s43630-022-00175-6

REVIEWS

Polymethine dyes for PDT: recent advances and perspectives to drive future applications

Degnet Melese Dereje[1,2] · Carlotta Pontremoli[1] · Maria Jesus Moran Plata[1] · Sonja Visentin[3] · Nadia Barbero[1]

Received: 30 September 2021 / Accepted: 15 January 2022 / Published online: 1 February 2022

Abstract

It has been proved that the effectiveness of photodynamic therapy (PDT) is closely related to the intrinsic features of the photosensitizer (PS). Over the recent years, several efforts have been devoted to the discovery of novel and more efficient photosensitizers showing higher efficacy and lower side effects. In this context, squaraine and cyanine dyes have been reported to potentially overcome the drawbacks related to the traditional PSs. In fact, squaraines and cyanines are characterized by sharp and intense absorption bands and narrow emission bands with high extinction coefficients typically in the red and near-infrared region, good photo and thermal stability and a strong fluorescent emission in organic solvents. In addition, biocompatibility and low toxicity make them suitable for biological applications. Despite these interesting intrinsic features, their chemical instability and self-aggregation properties in biological media still limit their use in PDT. To overcome these drawbacks, the self-assembly and incorporation into smart nanoparticle systems are forwarded promising approaches that can control their physicochemical properties, providing rational solutions for the limitation of free dye administration in the PDT application. The present review summarizes the latest advances in squaraine and cyanine dyes for PDT application, analyzing the different strategies, i.e.the self-assembly and the incorporation into nanoparticles, to further enhance their photochemical properties and therapeutic potential. The in vivo assessments are still limited, thus further delaying their effective application in PDT.

Degnet Melese Dereje and Carlotta Pontremoli contributed equally to this work.

✉ Nadia Barbero
nadia.barbero@unito.it

[1] Department of Chemistry, NIS Interdepartmental and INSTM Reference Centre, University of Torino, Via P. Giuria 7, 10125 Turin, Italy

[2] Department of Chemical Engineering, Bahir Dar Institute of Technology, Bahir Dar University, Polypeda 01, 0026 Bahir Dar, Ethiopia

[3] Department of Molecular Biotechnology and Health Science, University of Torino, Via Quarello 15/A, 10135 Turin, Italy

Graphical abstract

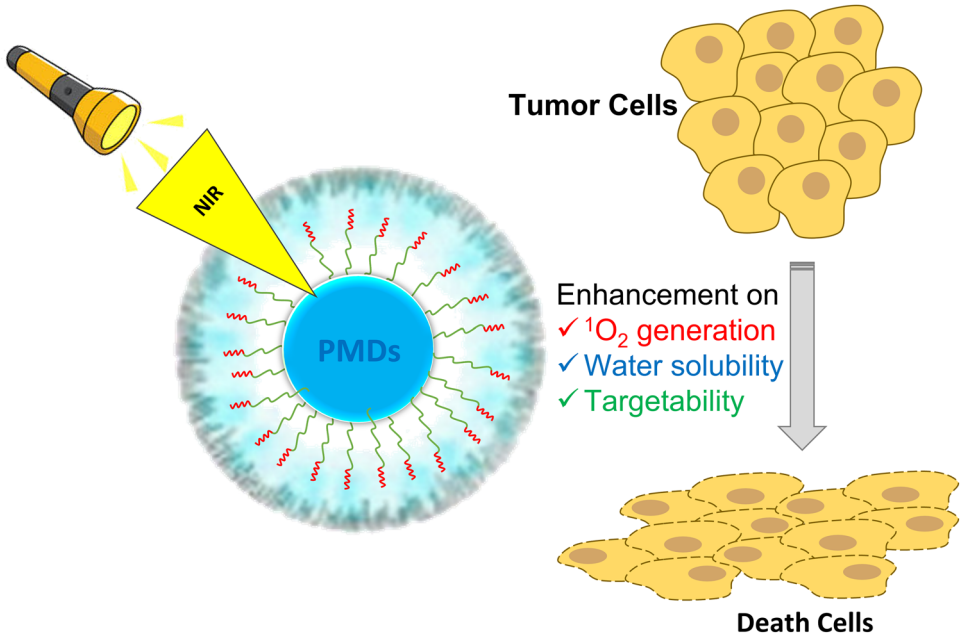

Keywords Photodynamic therapy · Polymethine dyes · Squaraines · Cyanines · Self-assembly · Smart nanocarrier

1 Introduction

The origin of photodynamic therapy (PDT), originally known as heliotherapy, dates back to ancient civilizations such as Egypt, Greece, China, Rome and India [1, 2]. At present, PDT represents an attractive technique for a wide range of applications, spanning from theragnostic [3, 4] and antimicrobial applications [5] to cancer therapies, as a promising alternative to the traditional treatments, thanks to the high selectivity for the target [6, 7] and the non- or minimal-invasive nature [6–9]. PDT involves three key factors, a photosensitizer (PS), light with an appropriate energy to penetrate the tissue window [10, 11], and molecular oxygen [12]. All these elements are harmless on its own but when the PS is excited by a non-thermal light (*i.e.* LED), at the appropriate excitation wavelength, reacts with oxygen, generating reactive oxygen species (ROS) which cause an oxidative damage responsible of the death of cells by necrosis and/or apoptosis [7, 12].

In fact, after the irradiation, the light is absorbed by the PS, causing the conversion from its ground state (singlet state, ^{1}PS) to an excited singlet state (^{1}PS*). Due to the instability of this excited state, the PS can lose the energy, returning to the ground state or, alternatively, the singlet state can undergo intersystem crossing (ISC), causing the spin conversion of the electron in the higher energy orbital and thus leading to excited triplet state (^{3}PS*). The triplet state is more stable and with a longer lifetime, allowing the energy transfer to molecular oxygen (O_2) (type II reaction mechanism) or the electron transfer to a substrate (type I reaction).

Moreover, PDT can be easily combined with other therapeutics [6, 11] and the side effects are relatively limited, showing cost effectiveness and higher cure rates [6, 12] compared to the traditional cancer therapies such as surgery, chemotherapy and radiotherapy [6, 9]. It has been proved that the effectiveness of PDT is closely related to the intrinsic features of the PS. Hence, designing PSs with red-shift excitation wavelength, high generation of singlet oxygen ($^1O_2$) and simultaneous selectivity to the target tumor is crucial for the therapy success.

To date, a plethora of photosensitizers have been developed and are currently used in PDT; based on progress of generation, they can be divided as first, second and third generation. The first generation includes porphyrins (Photofrin®) and chlorins, which have been widely clinically used in the treatments of lung, esophagus, pancreatic and bladder cancer. Despite their efficacy, some specific drawbacks related to hydrophobicity in biological microenvironment, non-specificity and poor tissue penetration due to light absorption at a specific spectral region led to the development of the second-generation photosensitizers (derivatives of chlorins, i.e Foscan®, bacteriochlorins, and phthalocyanines). This second generation of PSs showed a

stronger action on the tumor regions thanks to their strong absorbance in the Near-Infrared region (NIR), causing higher light penetration. With the aim to increase the selectivity, the third-generation PSs are based on the first and second-generation PSs conjugated with targeting molecules or encapsulated in biodegradable/biocompatible nanoparticles.

Among different NIR organic dyes, polymethine dyes (PMDs) are the most retaining attentions for wide application in various fields of science and technology: PDT [10, 13, 14], organic photovoltaics [15] and Dye-Sensitized Solar Cells [16, 17]. The advantage of PMDs over other classes of PSs relies in the possibility of easily tuning their structure to get the proper photophysical and photochemical properties for the desired applications [18, 19]. Even though the application of PMDs as PSs in PDT is limited compared to other classes of PSs such as phthalocyanines and most first-generation PS, porphyrins and their derivatives, the research interest in polymethine dyes for PDT is continuously growing during the last years, as reported in Fig. 1. In fact, thanks to their intrinsic photochemical properties such as broad absorption spectral range with high extinction coefficients and high fluorescence quantum yield (QY), summarized in Tables 1, 2 and 3, they could be considered as promising alternative PSs for photodynamic treatments. In addition, they can be synthesized with absorbance bands between 600 and 800 nm, perfectly fitting the phototherapeutic window, and the procedure to produce them allow to obtain a single pure compound under good manufacturing practice (GMP) conditions with quality control and low manufacturing costs. Finally, they possess a high singlet oxygen quantum yield leading to good production of ROS upon irradiation as well as no dark toxicity or side effects and relatively rapid clearance from normal tissues, minimizing the side effects of phototoxicity [20].

Despite the noticeable advantages related to the PDT technique compared with the conventional ones, currently, several drawbacks still limit its effective application, spanning from the convenient light source and photosensitizers' photophysical and chemical properties, such as the limited/poor water solubility in biological environment [21], to the low selectivity and the correct dose to exert the desired effect in vivo [22]. In particular, the poor water solubility of the PS results in a low fluorescence intensity due to self-quenching effect, leading to a reduction in the reactive oxygen species (ROS) generation.

Over the recent years, several efforts were devoted to overcome these limitations and to achieve higher solubility in biological fluids, a deep specificity of tumor microenvironment and hypoxic tumor [6, 21, 23], focusing the attention on the improvement of the PS photochemical properties to enhance the targeted PDT for cancer treatment.

In this review, we bring to light the recent advancements and future perspectives towards the potential of polymethine dyes as photosensitizers, specifically cyanines and squaraines, in PDT applications. A detailed structure to function analysis is defined in the first section. Due to some intrinsic limitation of these dyes, the second and third section is devoted to the self-assembly and incorporation into smart nanoparticle systems, as promising approaches to boost the dye efficiency. Finally, the overall recent in vivo studies on both cyanines and squaraines will be reported in the fourth and last sections, highlighting the lack of in vivo works and the limitation of the use of PMDs in therapeutic application.

2 Polymethine dyes

2.1 Squaraine dye-based photosensitizers

Squaraine dyes are four-membered ring systems derived from squaric acid through a dicondensation reaction of electrophilic aromatic moieties and squaric acid. Squaraines are characterized by sharp and intense absorption bands [20] and narrow emission bands with high extinction coefficients ($\varepsilon \sim 10^5$

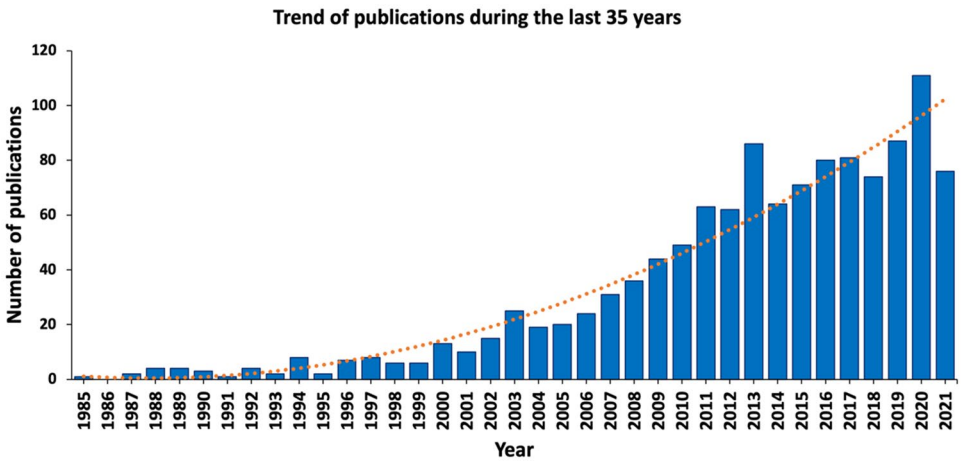

Fig. 1 Trend of the publications related to polymethine dyes over the last 35 years. (Source: SciFinder-n, Keywords: Polymethine dyes/Cyanines/Squaraines in Photodynamic Therapy and merging all the results)

Table 1 Summary of photophysical properties of the squaraine dye-based photosensitizers (**2a**–**2z**)

Comp	–R	Absorbance λ_{max} (nm)	Emission λ_{max} (nm)	PLQY	$^1O_2$ QY	References
2a		588[a]	–	0.02[c]	–	[35]
2b		610[a]/606[b]	621[b]	0.0003[b]	–	[36]
2c		617[a]/614[b]	630[b]	0.0002[b]	–	
2d		682[d], 663[e], 678[f]	705[d], 675[e], 683[f]	0.85[d], 0.21[e], 0.92[f]		[39]
2e		660[c], 667[g], 669[h], 671[i], 680[f], 687[j], 676[e], 651[k]	678[c], 682[g], 683[h], 684[i], 705[f], 703[j], 689[e], 665[k]	0.26[c], 0.42[g], 0.54[h], –[i], –[f], –[j], 0.29[e], 0.02[k]	–	[40]
2f		655[c], 659[g], 662[h], 664[j], 673[f], 680[j], 669[e], 643[k]	670[c], 674[g], 677[h], 678[j], 699[f], 695[j], 683[e], 658[k]	0.10[c], 0.20[g], 0.27[h], –[j], –[f], –[j], 0.17[e], 0.01[k]	–	
2g		605[c], 610[g], 610[h], 610[j], 617[f], 615[j], 608[e], 554[k]	665[c], 667[g], 664[h], 655[j], 684[f], 680[j], 670[e], 668[k]	0.20[c], 0.40[g], 0.48[h], 0.56[j], –[f], –[j], 0.30[e], 0.02[k]	–	
2h		685[l]	720[l]	0.47[l]	–	[43]
2i		670–690[l]	710–745[l]	–	–	
2j				–	–	
2k				–	–	
2l		668[e]	–		0.01[m]	[44]
2m		673[e]	–		0.03[m]	
2n		672[e]	–		0.03[m]	
2o		683[e]	–		0.06[m]	
2p		681[e]	–		0.08[m]	
2q		648[g]	662[g]			[10]
2r		655[g]	668[g]			
2s		638[g]	644[g]			
2t		640[g]	647[g]			
2u		659[g]	671[g]			
2v		643[g]	649[g]			
2w		645[g]	651[g]			
2x	R_1:CH_3	641[f]/619[n]	–		0.04[n]	[45]
	R_2:CH_2CH_3	642[f]/622[n]	–		0.05[n]	
2y	R_1:CH_3	652[f]/620[n]	–		0.27[n]	
	R_2:CH_2CH_3	645[f]/623[n]	–		0.16[n]	
2z	R_1:CH_3	659[f]/624[n]	–		0.14[n]	
	R_2:CH_2CH_3	660[f]/619[n]	–		0.36[n]	

[a]20% vol/vol ethanol–water (EtOH–H_2O)

[b]2% vol/vol methanol–water (MeOH–H_2O)

[c]Mmthanol (MeOH)

[d]Toluene

[e]Acetonitrile (ACN)

[f]Dimethylsulfoxide (DMSO)

[g]Ethanol (EtOH)

[h]Propanol (PrOH)

[i]Butanol (BuOH)

[j]dimethylformamide (DMF)

[k]Water (H_2O)

[l]H_2O:DMSO (from 60 to 80%)

[m]Chloroform (CFM)

[n]Dulbecco's modified Eagle medium (DMEM)

Table 2 Summary of all the photochemical properties of aminosquaraines (**4a**–**4z**)

Comp	–R	Absorbance λ_{max} (nm)	Emission λ_{max} (nm)	PLQY	$^1O_2$ QY	References
4a		648[g]		–	–	[14]
4b		657[g]				
4c		667[g]				
4d		658[g]				
4e		657[g]				
4f	Phosphorescence**	661[g]	1267**	0.02[e]	0.22[e]	[46]
4 g		670[g]	1265**	0.03[e]	0.26[e]	
4 h		679[g]	1267**	0.01[e]	0.09[e]	
4i		671[g]	1267**	0.11[e]	0.19[e]	
4j		682[g]	1267**	0.09[e]	0.16[e]	
4k	R=C_6H_{13} X=H	693[c], 605[f]		–	0.05[e]	[47]
4l		704[c], 631[f]			0.04[e]	
4m		705[c], 619[f]		–	0.03[e]	[48]
4n		715[c], 637[f]			0.05[e]	
4o		665[g]		–	0.29[e]	[51]
4p		675[g]			0.19[e]	
4q		684[g]			0.16[e]	
4r		676[g]			0.22[e]	
4 s		685[g]			0.10[e]	
4t	R = C_6H_{13}	684[a], 608[d], 658[b]		–	0.04[e]	[50]
4u		695[a], 617[d], 671[b]			0.06[e]	
4v	R_2=C_6H_{13}	651[c,f]		–	–	[53]
4w	R_2=C_6H_{13}	662[c], 660[f]				
4x	R_2=C_2H_5	647[c], 647[f]				
4y	R_2=C_2H_5	658[c], 657[f]				
4z	R_2=C_2H_5	657[c], 655[f]				

**Phosphorescence

[a]MeOH

[b]ACN

[c]DMSO

[d]Water (H_2O)

[e]CFM

[f]DMEM

[g]1% vol/vol dichloromethane–methanol (DCM–MeOH)

$M^{-1}cm^{-1}$) typically in the red and near-infrared region, good photo- and thermal stability and a strong fluorescent emission in organic solvents [24, 25]. Different reviews have been published reporting on squaraine dyes synthesis strategies [18, 26] and potential applications [19, 27, 28] including photoconductivity, data storage, optical detection [29], solar cells [17], bioimaging [24, 30], and photodynamic therapy [31–34].

2.2 In vitro PDT studies of squaraines

2.2.1 Phloroglucinol moiety

Even if squaraines have been proposed as photosensitizers since more than 20 years, few reports on their effective use as photosensitizers in cell cultures are present in literature. The first attempt is the work of Ramaiah and coworkers who analyzed the cytotoxicity and genotoxicity of three different squaraine dyes based on the phloroglucinol moiety [35] (**2a**–**c** in Fig. 2) already proposed as PS in 1997 [36]. The results showed that halogenated squaraines (**2b** and **2c**), and much less pronounced the non-halogenated dye (**2a**), exhibit

Table 3 Summary of the photophysical properties of cyanine dye-based photosensitizers (**5a**–**5g** and **6a**–**6l**)

Comp	Absorbance λ_{max} (nm)	Emission λ_{max} (nm)	PLQY	$^1O_2$ QY	References
5a	651[f]	671[f]	0.308[f]	0.003[f]	[59]
5b	654[f]	672[f]	0.086[f]	0.003[f]	
5c	651[f]	669[f]	0.059[f]	0.015[f]	
5d	686[b], 682[c]	705[b], 702[c]	0.302[c]	–	[60]
5e	689[b], 684[c]	709[b], 704[c]	0.291[c]	–	
5f	692[b], 688[c]	713[b], 709[c]	0.365[c]	–	
5g	689[b], 685[c]	709[b], 705[c]	0.381[c]	–	
6a	765[d]	827[d]	0.48[d]	0.75[d]	[62]
6b	783[a], 793[g], 775[h]	799[a], 817[f], 796[h]	0.041[a]	–	[69]
6c	790[e]	805[e]	0.22[e]	0.66[e]	[64]
6d	687[e]	780[e]	0.009[e]	0.44[e]	
6e	790[a], 800[d]	836[a]	–	–	[64]
6f	793[a], 802[d]	837[a]	–	–	
6g	796[a], 806[d]	844[a]	–	–	
6h	677[a], 675[h]	758[a], 753[h]	–	0.20[c]	[65]
6i	686[h]	759[h]	0.121[h]	0. 169[h]	[66]
6j	776[h]	820[h]	–	–	[67]
6k	781[a], 799[g], 779[h]	799[a],805[g], 800[h]	0.039[a]	–	[69]
6l	782[a], 796[g], 778[h]	804[a], 818[g], 791[h]	0.084[a]	–	[68]

[a]MeOH
[b]DMSO
[c]EtOH
[d]DMF
[e]H_2O
[f]Dichloromethane (DCM)
[g]10% Fetal bovine serum (FBS)
[h]Phosphate-buffered saline (PBS)

efficient cytotoxicity upon photoexcitation in two different mammalian cell lines. Moreover, the three dyes were found to be cytotoxic also in two strains of bacteria only after irradiation. On the same series of dyes, the same authors have analyzed the DNA damage and the cytotoxicity in mammalian cells and cell-free systems in presence and absence of various additives and scavengers [37]. This helped in understanding the mechanism of the process, indicating for instance the involvement of superoxide radicals and hydrogen peroxide for the two halogenated squaraines while the photobiological activity of the non-halogenated ones seems to be mediated by type-I reactions.

More recently, the diiodo-squaraine (bis(3, 5-diiodo-2,4,6-trihydroxyphenyl)squaraine) (**2c**) showed a maximum photodynamic activity in human breast cancer cells MDA-MB-231 compared to other cancer cells (oral, cervical, colon and pancreatic) with a very little cytotoxicity in normal breast cells MCF-10A [38]. The authors applied a proteomic approach who revealed that PDT induces oxidative stress and initiates a series of pro and anti-apoptotic pathways, including cell redox homeostasis, response to unfolded protein response, regulation of programed cell death, actin cytoskeleton organization and cell redox homeostasis in breast cancer cells. They concluded that this PS could be a good candidate for PDT since it induced a predominant apoptotic cell death pathway rather than necrosis with lesser damage to surrounding healthy cells.

2.2.2 Benzothiazole moieties

In search for a wider absorption in the tissue transparency window, Rapozzi et al. introduced the *N*-alkylbenzothiazole residue on two squaraines, each containing two C6 hydrocarbon chains that might favor their association to the cell membranes [39]. The two proposed PSs show absorption between 550 and 750 nm (with Abs peaks around 660–680 nm), almost perfectly matching the so-called "phototherapeutic window" (600–900 nm) and their photodynamic effect was tested in four cell lines. As shown in Fig. 3, the symmetric dye **2d** resulted a strong photokilling agent at relatively low concentration ($\leq$ 1 μM). The proposed photooxidation process is through a type I mechanism, through the formation of peroxide and hydroperoxide species, leading to cell death primarily by necrosis. Moreover, these molecules efficiently internalize in HeLa cells and accumulate in the cytoplasm, as shown by confocal microscopy studies (Fig. 3).

Few years later, Shafeekh et al. [40] proposed three water-soluble bisbenzothiazolium squaraine dyes. A structure–activity study was performed indicating that the dye with iodine substitution (**2e**) on both benzothiazolium units was the best performing one, compared to the SQMI (**2f**) with only one iodine substitution. The symmetrical diiodinated dye (**2e**) resulted an efficient PS for PDT also in in vivo cancer models [41, 42]. The less active dye was the unsymmetrical squaraine dye ASQI (**2g**) containing iodinated benzothiazolium and aniline substituents confirming that the presence of iodine and sulfur atoms in these molecules can improve its intersystem crossing efficiency to the triplet state. Photodynamic effect with these dyes was expected to be through the generation of both singlet oxygen (type II) and ROS (type I).

A further modification of benzothiazole-based dyes was proposed by Wei et al. [43] with a dicyanomethylene substitution on the central four-membered ring making them potential NIR PSs with absorption between 600 and 700 nm. The authors proposed four different structures (**2h**–**k**) where the alkyl chain nature was modified to understand

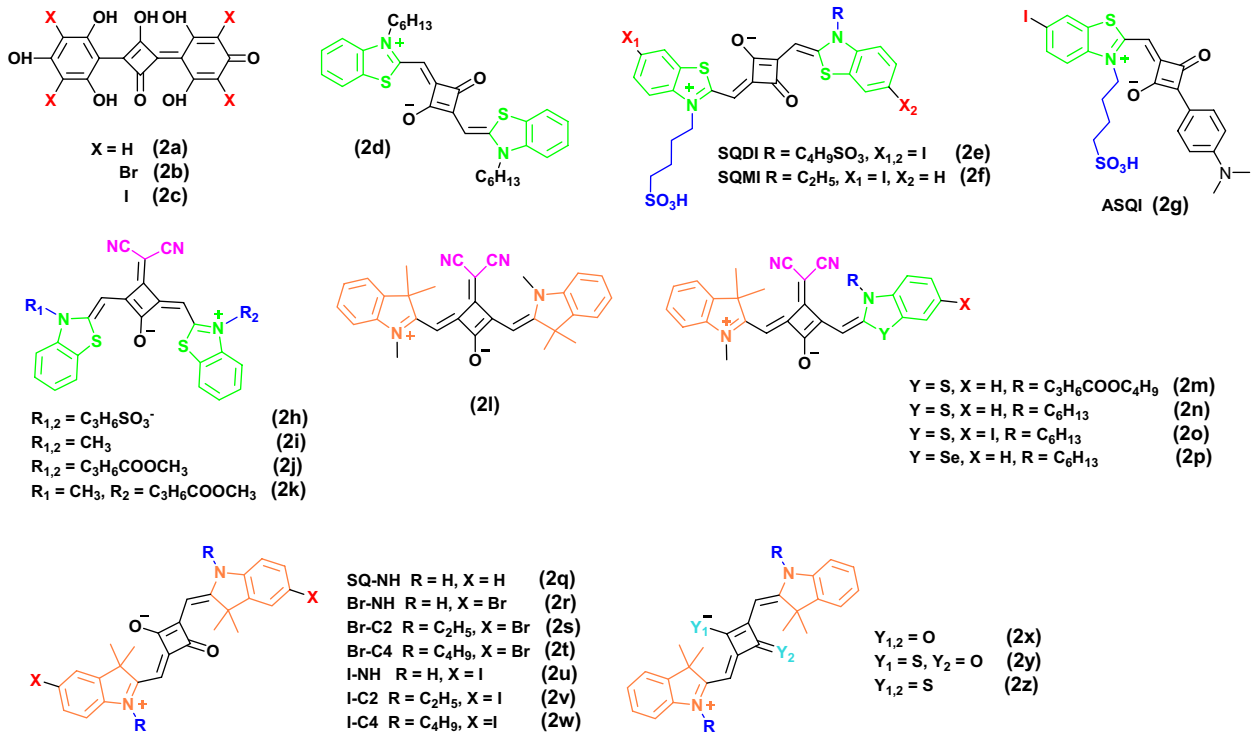

Fig. 2 Molecular structures of squaraine dyes

its effect on the biological activity. The dicyanomethylene-substituted benzothiazole dye carrying two sulfonic groups (**2h**) was not able to enter the cell membranes, while lysosomes location was obtained for the other squaraines where these groups were substituted with electrically neutral methyl or methyl butanoate groups.

2.2.3 Dicyanomethylene squaraines

A similar structure-function approach was proposed by Martins et al. [44] on a series of symmetrical and asymmetrical dicyanomethylene squaraines with different lateral substituents: indolenines (**2l**), benzothiazole (**2m–o**) and benzoselenazole (**2p**) groups. This latter showed the best activity causing a decrease in cell viability greater than 30% despite the very low singlet oxygen QY suggesting a type I reaction mechanism.

2.2.4 Indolenine-based squaraines

Squaraines with differently substituted indolenine moieties (**2q–w**) have been obtained via a one-pot condensation reaction by Serpe et al. [10]. Results observed that not only the presence of bromine (Br-C2, Br-C4) or iodine (I-C2, I-C4) on the indolenine ring facilitates the inter-system crossing, but also their hydrophilic–lipophilic balance strongly affects the pharmacological activity. Moreover, confocal studies showed the effective intracellular localization of Br-C4 and I-C4 squaraine dyes inside HT-1080 cells in cellular mitochondria. The insertion of one or two sulfur atoms on the central core (**2x–z**) was able to increase the singlet oxygen generation efficiency decreasing the photostability of the dyes [45].

All the photochemical properties of the above-mentioned squaraines (**2a–2z**) have been collected and reported in Table 1.

2.2.5 Aminosquaraines

Aminosquaraines, or squarilium cyanine dyes, are a particular class of cationic squaraines in which one of the oxygen atoms of the central four-member ring has been replaced by an amino group. In this way, these dyes possess a positive charge and a cationic character that may facilitate the cellular uptake. Moreover, the presence of the electron-donating amino group, in addition to improving their solubility in physiological conditions, may increase the rigidity of the central bridge and consequently raising the efficiency of singlet oxygen generation [46].

The first report on the in vitro photosensitizing ability of symmetrical aminosquaraine dyes was published in 2017 [14] where a series of differently substituted symmetrical benzothiazole aminosquaraines (**4a–e** in Fig. 4) were

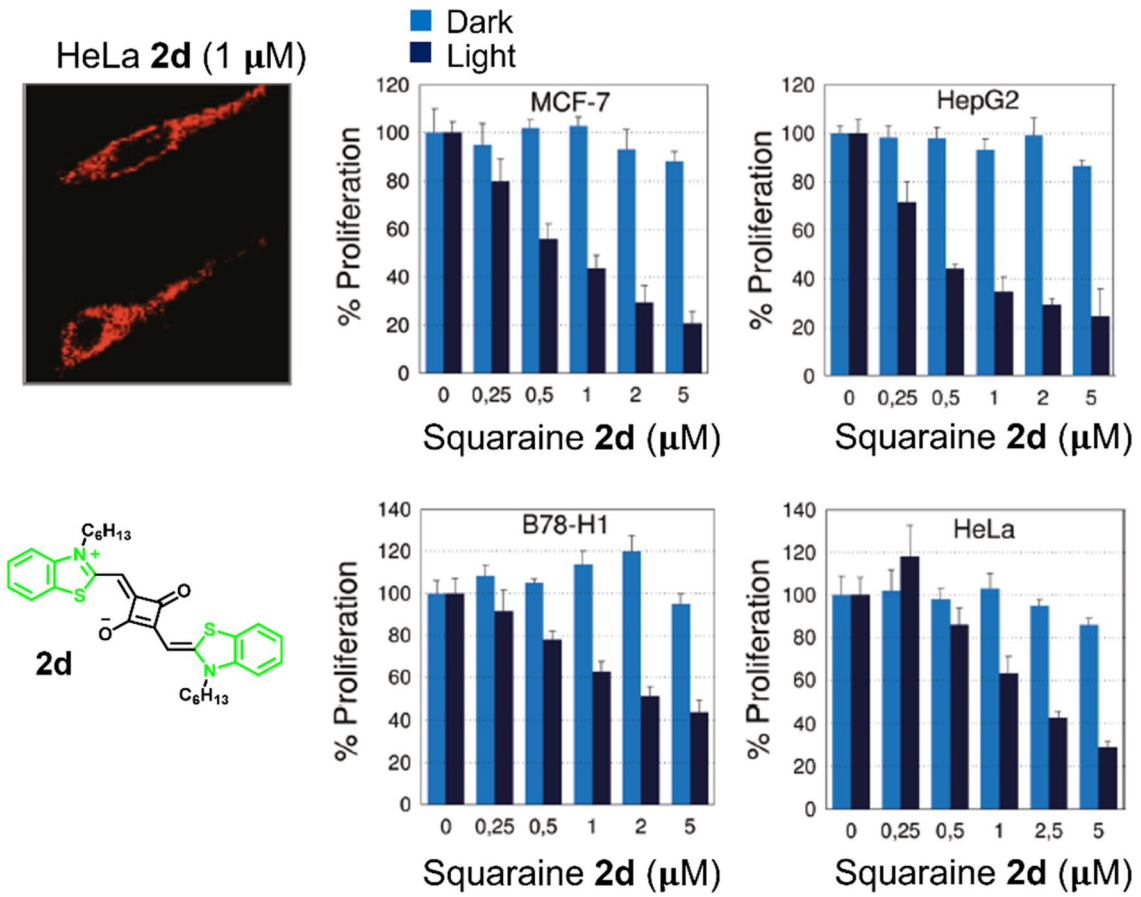

Fig. 3 (Up left) Confocal laser microscopy images of HeLa cells treated for 4 h with squaraines **2d** (1 μM). (Right) Cytotoxicity of increasing amounts of squaraine **2d** delivered to four different cancer cell lines either in the dark (light blue) or after light treatment (fluence rate, 15 J cm^{-2}) (dark blue). Viable cells were measured with a resazurine assay. Histograms report in ordinate the percent of relative proliferation, that is, the ratio RFUT/RFUC 100, where RFUT is the fluorescence of treated cells, while RFUC is the fluorescence of untreated cells. The data are the means of three independent experiments. Modified and reprinted with permission from Rapozzi et al. [39]. Copyright (2010) American Chemical Society

synthesized and tested in several human tumor cell lines. All compounds showed to inhibit the tumor cells upon irradiation but with a non-negligible cytotoxicity in the dark. A couple of years later, the same group inserted a heavy atom (*i.e.* iodine) on the benzothiazole ring (**4f–j**) slightly shifting the absorption (+ 10 nm) towards the NIR region and increasing the singlet oxygen quantum yield [46]. When compared to the non-halogenated analogues, these symmetrical diiodinated benzothiazole aminosquaraines exhibited, in general, lower Growth Inhibition GI_{50} values under irradiation. A further structural modification was introduced by the development of asymmetrical aminosquarylium cyanine dyes derived from benzothiazole and quinoline (**4k** and **4l**) [47]. The presence of a moiety of quinoline shifts the maximum absorption wavelength to NIR region (λ_{max} 693–704 nm). However, their dark toxicity is higher respect to the non-modified squaraine dye. A further modification was obtained by the introduction of an iodine atom into the quinoline heterocycle (**4m** and **4n**) (λ_{max} 705–715 nm) [48]. This modification did not increase the ROS production but significantly improved the in vitro phototherapeutic activity, suggesting a type I reaction mechanism. Unfortunately, a complete comparison is not possible since the reported compounds show the same structure but different counterions (I^- vs $CF_3SO_3^-$): the external heavy atom effect should increase the singlet oxygen quantum yield by about 20% [49]. An increase of cytotoxicity was recorded for symmetrical (**4o–s**) and asymmetrical benzoselenazole aminosquaraines (**4t** and **4u**) [50, 51]. They exhibited photodynamic activity against different human tumor cell lines, inhibiting cellular growth upon exposure to light mostly with GI_{50} values less than 5 μM. In general, these compounds are more cytotoxic than their benzothiazole analogues and showed inhibitory activity in the dark. Indolenine-based aminosquaraine dyes (**4v–z**) were highly cytotoxic in all radiation

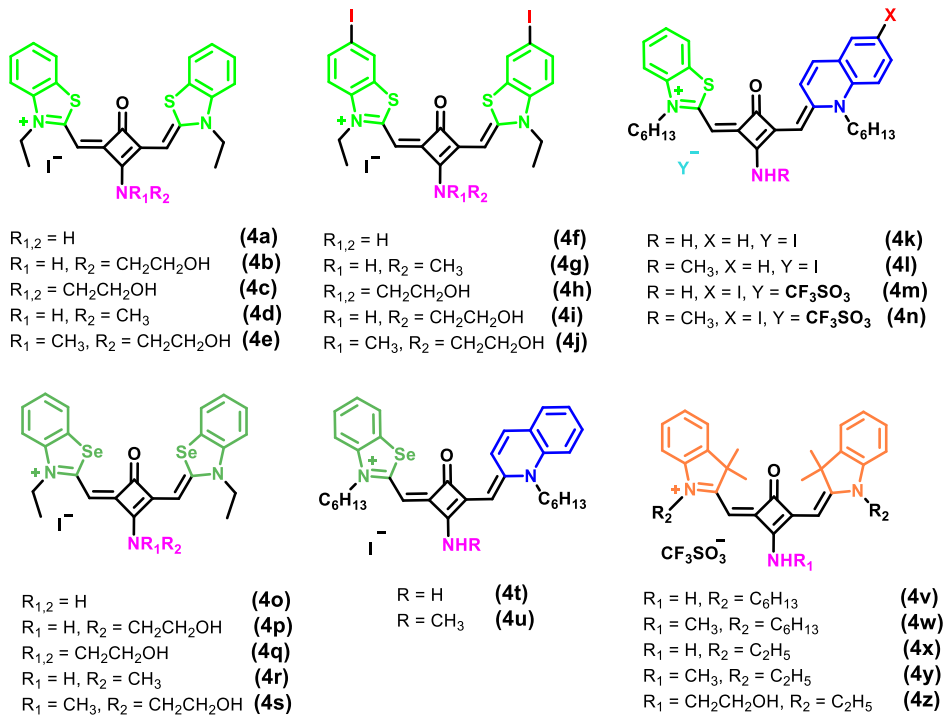

Fig. 4 Molecular structures of aminosquaraine dyes

conditions and also in the dark and therefore are not of interest as PDT photosensitizers [52, 53].

From all these studies, it is not clear the real influence of the counterion and chain length on the photodynamic activity. In all the examples reported in literature, if we compare these compounds with the squaraine counterpart, the introduction of the amine group into the central ring always increases the dark cytotoxicity.

2.2.6 Cyanine dye-based photosensitizers

Cyanines belong to the polymethine dyes family: their structure is characterized by two nitrogen heterocyclic rings (i.e. pyridine, indolenine, benzoindolenine, imidazole, benzothiazole, quinoline) connected via a π-conjugated chain. This chain is constituted of sp^2-hybridized carbon atoms. Depending on the number of methine groups of this chain, cyanines can be categorized as monomethine (Cy1), trimethine (Cy3), pentamethine (Cy5) or heptamethine (Cy7) cyanines [54].

Cyanine dyes have been widely investigated due to their excellent properties that make them suitable for a wide variety of applications. First of all, their absorption maxima can be tuned to the NIR region through easy structural modifications. Moreover, their biocompatibility, low toxicity and good photostability make them suitable for biological applications and in particular for photodynamic therapy [6, 33, 55–58].

2.3 In vitro PDT studies of cyanines

2.3.1 Pentamethine cyanine dyes

Pentamethine cyanine dyes possess long absorption wavelength perfectly within the phototherapeutic window. Huang et al. [59] proposed three symmetric indolenine-based

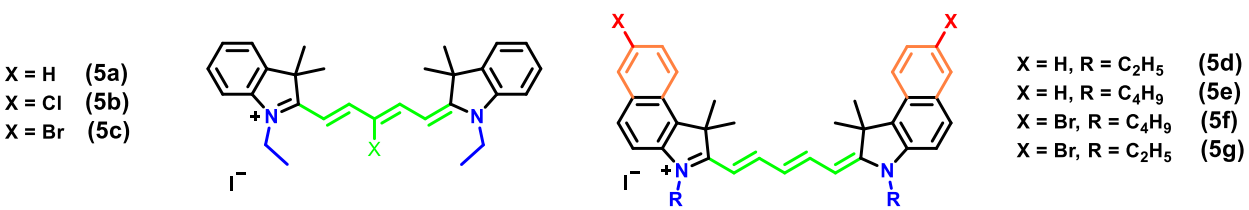

Fig. 5 Molecular structures of pentamethine cyanine dyes

penthamethine cyanines (**5a**–**c** in Fig. 5) with different halogen groups on the central (meso) position (λ_{max} = 651–654 nm). Among these three dyes, the Br-substituted one was able to enhance the singlet oxygen quantum yield showing a better half maxima Inhibitory Concentration IC_{50} and higher phototoxicity against MCF-7 cells with mitochondria localization. Our group reported a series of symmetrical Cy5 based on the benzoindolenine ring with different substitutions: bromine and C2 or C4 alkyl chains (**5d**–**g**) [60]. These PSs have an absorption slightly more shifted toward the NIR (680–699 nm) with phototoxicity at very low concentration (10 nM). Surprisingly, the presence or absence of the heavy atom was not highly affecting the PDT activity which was slightly higher for longer alkyl chain dyes.

2.3.2 Heptamethine cyanine dyes

Compared to pentamethine with the same functional groups, heptamethine cyanine dyes have a maximum absorbance shifted to the near-infrared range of around 100 nm. The most used Cy7 is without any doubt Indocyanine Green (ICG), reported in Fig. 6. Among its advantages, water-solubility and biocompatibility along with excellent photochemical properties made it one of the most used cyanines in the biomedical field: ICG is the only Food and Drug Administration (FDA) approved NIR agent as imaging probe. ICG also shows some disadvantages like poor aqueous stability, rapid body clearance and lack of targeting properties. For PDT applications, one of the most drawbacks is its low singlet oxygen QY and the very low activity as PDT PS [61].

The examples of Cy7 applied in PDT are modification of the ICG skeleton as attempts to improve the PDT efficacy: Cao et al. introduced iodine atoms on the indolenine ring (**6a** in Fig. 6) to improve the ROS production [62]. This novel symmetrical iodine NIR Cy7 (λ_{max} = 749 nm) could generate singlet oxygen along with heat indicating that it can be an ideal phototheranostic agent for a synergistic photodynamic and photothermal (PDT/PTT) treatment for deep tumors. In this case, the effect of iodination was evident in increasing cancer cell apoptosis and inhibition rate in deep HepG2 tumors.

Like this example, most of all the compounds present in literature are modifications of ICG to get more efficient PS

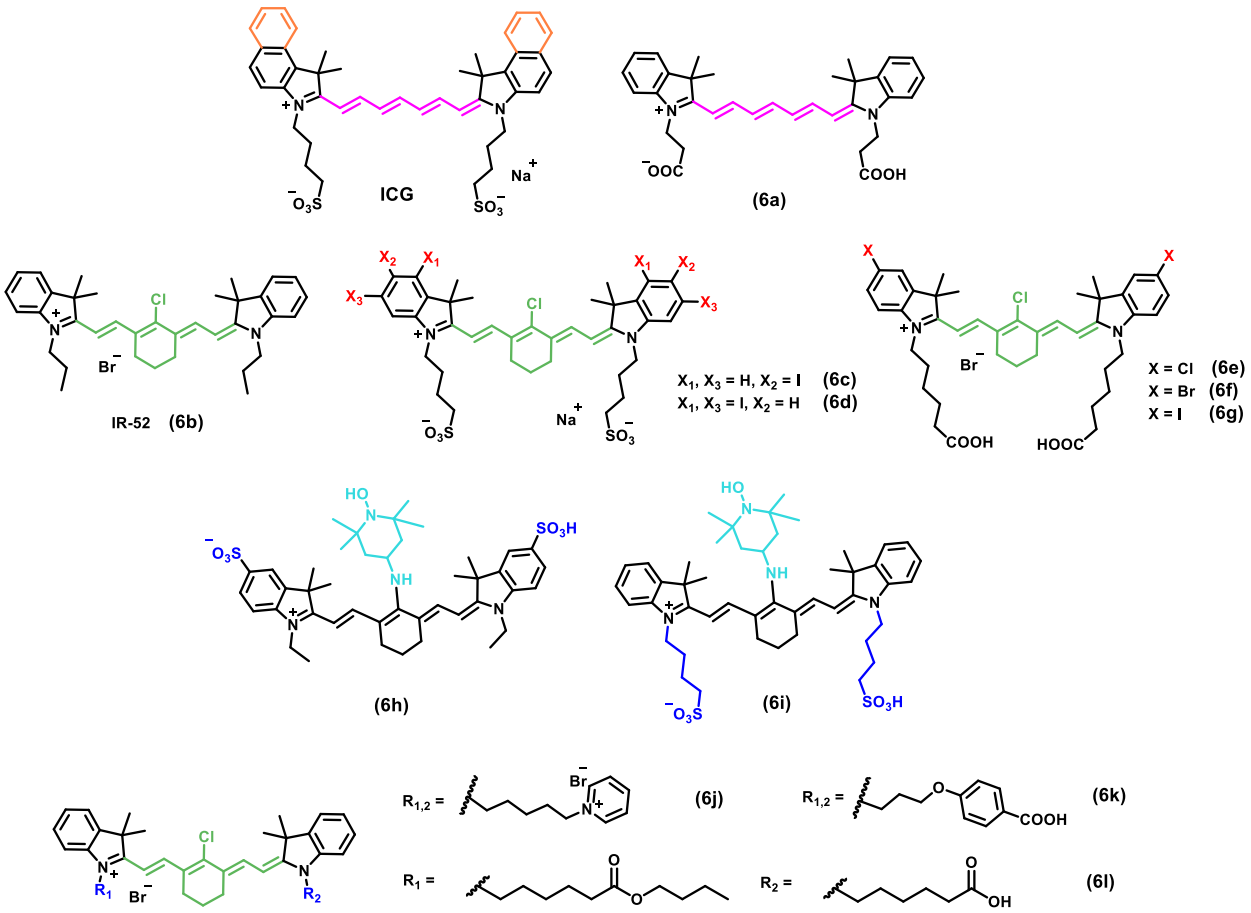

Fig. 6 Molecular structures of heptamethine cyanine dyes

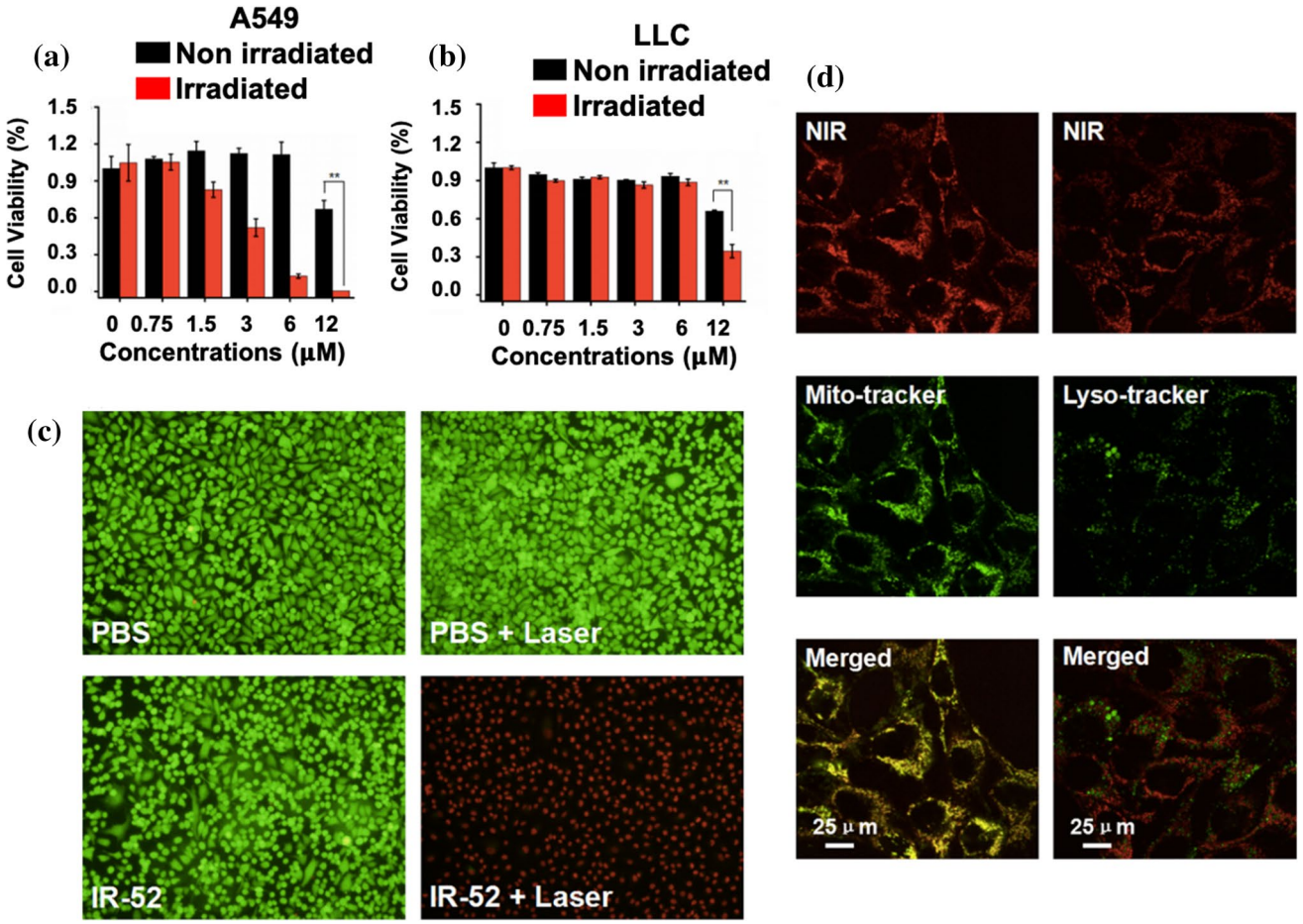

Fig. 7 In vitro cytotoxicity induced by phototherapy and mitochondrial localization. **a**, **b** Viabilities of A549 and LLC cells after incubated with different concentrations of IR-52 (**6b**) for 24 h exposed to laser irradiation (808 nm, 2 W cm^{-2}) or not for 5 min. **c** Fluorescent images of Calcein AM/PI co-stained A549 cells after different treatments (green: Calcein AM, red: PI). **d** Mitochondrial localization was determined by co-stained IR-52 with Mito-tracker in A549 cells. Lyso Tracker Green was used as a negative control. Image obtained from the work of Chen et al. [63]. This image is licensed under a Creative Commons Attribution 4.0 (CC-BY) International Licence

maintaining or trying to maintain the impressive ICG fluorescence characteristics. All the Cy7 proposed as PSs are based on the indolenine ring instead of benzoindolenine one as in ICG and most of them are designed with the polymethine bridge stabilized by a cyclohexene moiety, substituted by a chlorine atom.

Chen et al. synthesized a lipophilic cationic Cy7 (IR-52, **6b**) with mitochondria localization and absorption maxima at 789 nm [63]. Even if IR-52 does not bear any heavy atoms, this simple symmetrical indolenine-based Cy7 exhibited high phototoxicity against A549 cells and tumor-targeted in vitro and in vivo PDT and PTT efficacy, as clearly highlighted in Fig. 7.

The dye modification with the insertion of heavy atom, to get more efficient PSs, can greatly affect the photophysical properties, as demonstrated by Atchinson et al. [61] who prepared two iodinated derivatives with mono- and di-iodinated indolenines (**6c** and **6d**). They proved that the addition of two atoms of iodine on the indole ring dramatically quenches the fluorescence emission with a significant blue shift while the presence of only one iodine greatly improves both singlet oxygen production and PDT efficacy.

To better understand the effect of the heavy atom on the photophysical properties and photodynamic activity, a structure-function study was reported by Meng's group where a series of symmetrical indolenine-based halogenated Cy7 has been synthesized by changing the nature of the halogen (chlorine, bromine and iodine, **6e**, **6f** and **6g**, respectively) [64]. The authors showed a positive correlation with the increase of the atomic number of halogen atoms as far as photochemical properties and photothermal stability are concerned but not for singlet oxygen QY and PDT activity.

Another way to increase the singlet oxygen quantum yield is the insertion of 2,2,6,6-tetramethylpiperidinyloxy (TEMPO) which is known to enhance the inter system

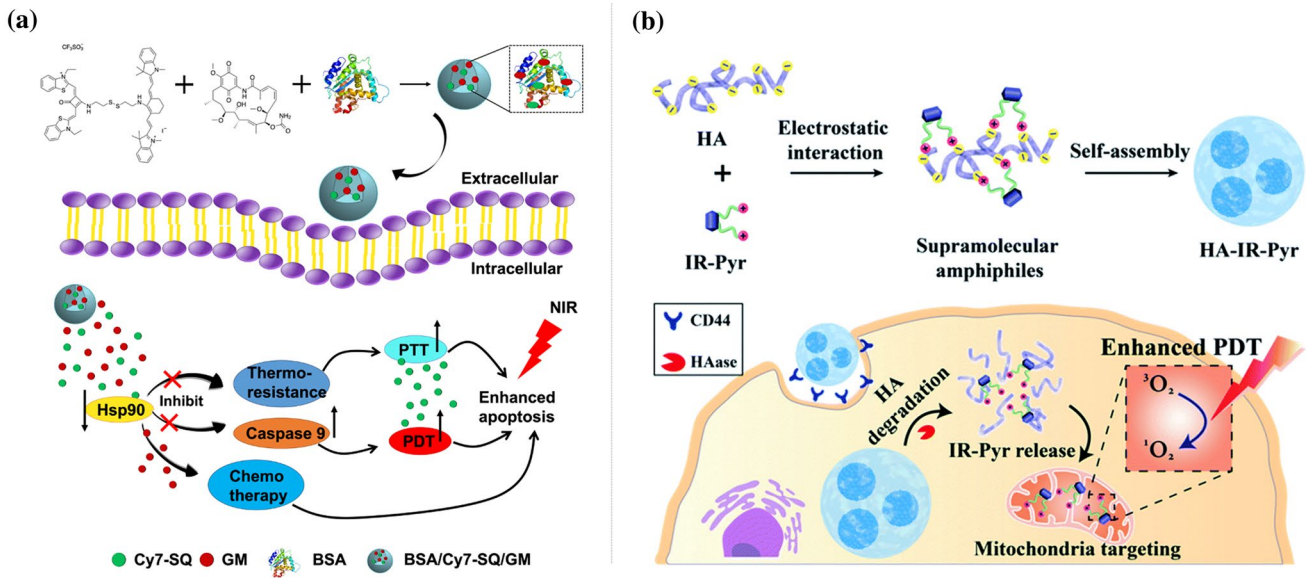

Fig. 8 **A** Schematic representation of the self-assembled BSA/Cy7–SQ/GM NPs for Hsp-90-regulated synergistic PDT/PTT combined with chemotherapy [70]. **B** Illustration showing the formation of HA-IR-Pyr, receptor mediated (CD44) cellular uptake and cancer-mitochondria localization for enhanced PDT. Reproduced from [67] with permission from the Royal Society of Chemistry

crossing (ISC) process. Two different studies have proved the efficacy of this strategy both introducing TEMPO on the central bridge of two water-soluble Cy7. The resulting symmetrical indolenine-based dyes, with sulfonic acid moieties on the ring (**6h**) [65] or on the alkyl chains (**6i**) [66], showed an increased Stokes shift, high singlet oxygen quantum yield, very low dark toxicity, high chemical stability and excellent properties in PDT process.

Among the main problems to overcome, the dye solubility and targeting ability are the most urgent to solve. The first can be dealt with the introduction of groups that can increase water solubility and prevent aggregation such as sulfonic acid moieties on the ring [65] or on the alkyl chains [66], pyridinium ion into the alkyl chains [67], (**6j**) thus providing increased photostability and dye performances. Moreover, the possibility of inserting different functional groups on the cyanine skeleton could be useful for the interaction and/or covalent binding of these dyes with targeting molecules and/or proteins, thus, leading to a preferential accumulation at tumor sites and selective accumulation in the mitochondria of cancer cells (**6j**, **6k**, **6l**) [67–69].

All the photochemical properties of the above-mentioned pentamethine (**5a**–**5g**) and heptamethine (**6a**–**6l**) cyanines have been collected and reported in Table 3.

3 Self-assembly

As already mentioned, despite the ability of PMDs to generate ROS and their photochemical properties suitable for the PDT process, both cyanines and squaraines suffer from poor water solubility, aggregation in aqueous media and altered photophysical, photo-chemical and biological properties. Over the recent years, inspired by living organisms, self-assembly has emerged as a process in which small, disordered parts build an organized final challenging molecular structure. Based on this strategy, researchers are moving in search of self-assembled PS systems with tumor-targeting ability with the aim of increasing the efficiency of the treatment and minimizing the PS toxic side effects to the healthy tissues.

3.1 Self-assembly of squaraines

To the best of our knowledge, the only example of a squaraine dye used as self-assembled PS for PDT has been reported by Wen et al. [70]. They designed a Cy7–SQ system by a covalent disulfide linkage between the Cy7 used as photothermal agent and the SQ as photosensitizer to improve the photostability and thermal stability of both dyes (Fig. 8A). To further increase the therapeutic efficiency, geldanamycin (GM), an anticancer agent, was exploited to prevent the undesirable overexpression of surviving Hsp-90 in cancer cells. Thus, a self-assembly of BSA/Cy7-SQ/GM nanoparticles were designed to achieve Hsp-90-regulated synergistic PDT/PTT combined with chemotherapy. When entering in

contact with the glutathione present in the tumor-microenvironment, the covalent-disulphide link from the SQ-Cy dye will be broken in the corresponding photosensitizer and photothermal agents, allowing the simultaneous generation of ROS and heat for an efficient synergistic effect.

3.2 Self-assembly of cyanines

The literature on the self-assembly involving cyanines is plenty of examples compared to squaraines. Li et al. [71] have recently described a non-symmetrical Cy3 that can assemble into a smart J-aggregate system, under the regulation of negative charged microenvironment. Once injected intravenously, Cy J-aggregates reached the tumor site exploiting the EPR effect. After the cell internalization, the negatively charged microenvironment, provided by intracellular RNA, stabilized once more the J-aggregates. Compared to the free dye, the PS J-aggregate enhances the singlet oxygen QY inducing a bathochromic effect in absorption and fluorescence emission spectra (λ_{max} free iodide-cyanine: 630 nm vs λ_{max} J-aggregates: 700 nm), moving to an optimal wavelength for the PDT treatment and thus improving the PDT efficiency.

New target-strategies have been designed taking advantage of the abnormally overexpression of some peptides or glycoproteins in the cancer microenvironment. For instance, glutathione (GSH) is a peptide mostly expressed in cancer cells and it has been used by Jeong and coworkers [72] for designing a new multi-functional drug delivery system for PDT, based on a fluorescent color-changeable branched-form heptamethine cyanine dye (PEG-4-CyP). The amphiphilic structure of PEG-4-CyP is able to assemble in a nanoparticle-like structure by encapsulating the doxorubicin (DOX), a chemotherapy drug used to treat cancer. This system exhibited a change in the maximum absorbance wavelength from 650 to 795 nm after the reaction with GSH. Simultaneously, the glutathione is able to reduce the non-native disulphide bonds, letting the DOX release.

Recently, targeting mitochondria has also become an intelligent therapeutic strategy able to overcome the hypoxia factor of PDT, resulting in a higher healing-efficacy. Indocyanines dyes, particularly IR-780 derivatives, are known for their mitochondria-targeting ability and good absorption range. However, the inherent dark toxicity and low dye-dose tolerant, the low solubility in aqueous solutions and the fast photobleaching limit the therapy efficacy. Hence, as an alternative, encapsulation of the PS within a hydrophobic core of a polymeric or lipid-based nanocarrier can be used as a general strategy. In this context, Yuan and coworkers [73] developed in 2015 a water-soluble and highly stable self-assembled IR-780 containing dye. The novel structure was obtained by modifying the aliphatic chain of IR-780 from C3 to C16, providing a better self-assembly capacity with hydrophilic PEG_{2000}. Following a similar strategy, Thomas et al. [67] reported in 2017 a highly-soluble water-stable indocyanine derivative (**6j**). To improve the cancer selectivity, a self-assembly strategy was designed, and a supramolecular polymer was built using electrostatic interaction between the positively charged IR-Pyr and the negatively charged hyaluronic acid (HA) polymer (Fig. 8B).

Actually, HA, a negatively charged biocompatible polysaccharide molecule, has shown good ability to target cancer cells binding to the CD44 receptors overexpressed on the surface of the tumor [67]. In the same way, IR-780 loaded nanoparticles based on folic acid modified chitosan (FASOC-IR780 NPs) has been developed by Yang et al. [74]. The self-assembled NPs showed notable targeting and theragnostic potential in breast cancer therapy with a single NIR laser irradiation. A similar strategy has been developed [75] successfully combining cancer imaging and multiple phototherapy functionalities. In this case, they constructed a novel theragnostic nanocarrier (HA-PEG-CyI, hereafter called HPC) by inducing the self-assembly of PEGylated iodinated-cyanine dye (CyI) and attaching the ligand to its surface. The prepared HPC showed excellent synergistic photo- and photothermal properties, being able to generate both reactive oxygen species (ROS) and increase temperature under 808 nm laser irradiation, therefore, inducing apoptosis and necrosis in the tumor site. Indeed, the combination of PDT/PTT nanomedicine has been significantly improved during the last years compared to a single phototherapy modality, which often has shown limited therapeutic efficacy in vivo. Moreover, the appreciable local hyperthermia created by PTT increases intratumoral blood flow and oxygenation, which is favorable for the PDT, showing a synergetic effect of both therapies when applied at the same time.

As already stated in Sect. 1.4.2, ICG has been widely used as a prototype structure to design analogue molecules. In this context, in 2016, Miao and coworkers [76] designed the synthesis of PEGylated cypate, which in aqueous solution spontaneously self-assembled into micellar-type nanoparticles (SP^3NPs, ≈ 60 nm) with the cypate in the particle core and the hydrophilic PEG towards water. The irreversible decomposition of the particles undergoes upon NIR irradiation allowing to simultaneously generate both singlet oxygen for PDT and heat for PTT. Moreover, as a potential nanomedicine, SP^3NPs exhibit intense NIR florescence (more than three-fold stronger intensity than the free cypate) after irradiation at 800 nm, suggesting the possibility of deeper tissue penetration. In 2017, Tan et al. [68] used ICG as a prototype structure to develop for the first time a new analog, IR-DBI, with simultaneous cancer-targeted, NIR imaging and chemo-/PDT/PTT/multimodal anticancer activity. The ICG structure was modified by inserting a rigid cyclohexenyl in the middle of the polymethine linker and by changing the two N-alkyl side chains with a water-soluble carboxyl group and a lipo-soluble ester. This asymmetrical and amphipathic structure was afterwards

self-assembled with human serum albumin (HSA) to obtain spherical-nanosized HSA@IR-DBI complexes with 66.7% of encapsulation efficiency and very small diameter (15 ± 5 nm), facilitating its tumor-preferential accumulation through the EPR effect. Under NIR laser irradiation (≈ 808 nm, 1.5 W cm^{-2}, 5 min), this drug-protein complex as well as IR-DBI, caused hyperthermia and high ROS generation in aqueous solution as well as in cancer cells.

Peroxynitrite ($ONOO^-$) has been proved to be an efficient oxidizing and nitrating agent with high toxicity to cells than most free radicals. In this context, Zhang et al. [77] developed a strategy in which a novel NIR-triggered Cy7-block copolymer that was self-assembled in aqueous solution with N-nitrosated naphthalimide (NORM) to form a dye-based polymer nanoplatform. Under 808 nm light irradiation, these particles are not only able to generate ROS ($^1O_2$ and $O_2^{\cdot-}$) and heat, but also a large amount of NO gas, thereby the in situ formation of $ONOO^-$ that enhances photodynamic and photothermal therapy.

4 Smart nanocarriers

This section is devoted to a systemic review of organic (polymer- and protein-based), inorganic (SiO_2, ZnO, Fe_2O_3, Au, MnO_2) and hybrid and multifunctional NPs exploited to overcome the abovementioned limits of free PSs and to enhance targetability, singlet oxygen production, solubility and stability of free dye administration in PDT application under different stimuli [78–81], as illustrated in Fig. 9.

On the one hand, organic nanocarriers have attracted considerable attention for drug delivery due to its biocompatibility and biodegradability, well-described versatile functionalization, and formulations and methods of production adapted to various types of hydrophilic or hydrophobic drugs [78, 82]. On the other hand, inorganic and hybrid materials retained attention in imaging guided therapy thanks to its inertness, stability and above all good optical and magnetic properties [83].

4.1 Squaraine-based NPs

The literature on nanocarrier systems for squaraine dyes delivery in PDT is still limited. In fact, there are few inorganic and hybrid nanocarriers used to surmount the shortcomings of administering free squaraines. Among them, mesoporous silica nanoparticles (MSNPs) can be easily exploited to this purpose thanks to their high surface area and pore volume [84]. Sreejith et al. [85] designed a nanocarrier based on MSNP combined with graphene oxide (GO) and incorporating a phloroglucinol squaraine dye (**2a**). The physical isolation exerted by GO nanosheets protects squaraines from nucleophilic attack allowing the internalization of the dye into HeLa cells. Also Miletto et al. [86] incorporated different Br substituted indolenine-based squaraine dyes (**2r–t**) into MSNPs and assessed ROS release.

Semiconducting zinc oxide NPs is another hybrid smart nanocarrier which showed an interesting enhancement of squaraine photochemical and physicochemical properties such as singlet oxygen production, aggregate quenching behavior and pH responsiveness. Charge transferring phenomena occur at the interface junction while the squaraine is adsorbed on the NPs surface which is responsible to improve the ROS generation ability [87]. Remarkably, the study confirmed three times increase of singlet oxygen generation compared to free dye in vitro.

In a very recent paper, a theragnostic nanoprobe composed by a symmetrical dicyano indolenine-based SQ and a DSPE-PEG-modified ultrasmall superparamagnetic iron oxide NPs labeled with a green fluorophore (naphthalimide,

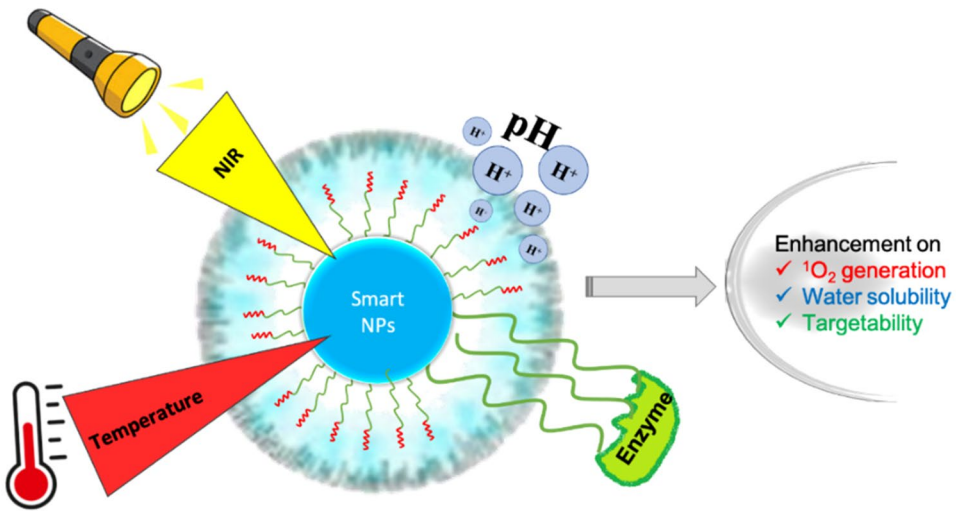

Fig. 9 Multifunctional responsive smart nanoparticle to enhance therapeutic application

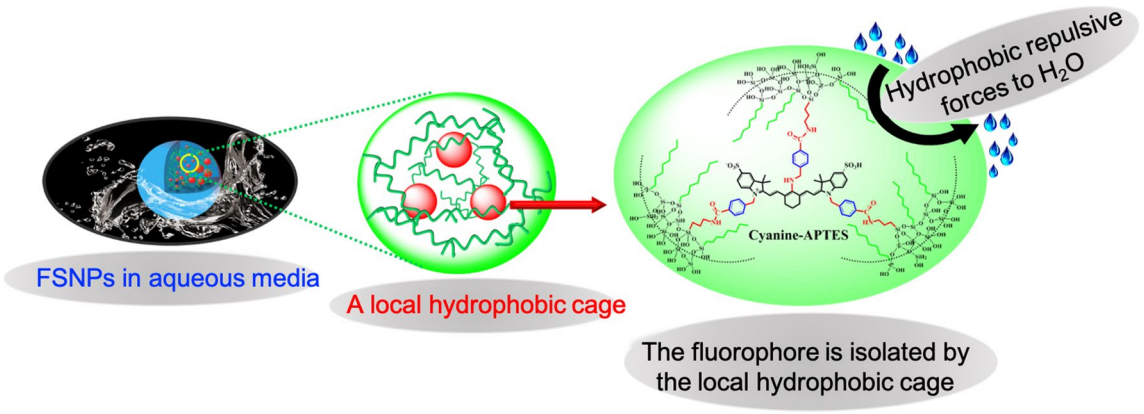

Fig. 10 Simplified representation of a local hydrophobic cage inside cyanine-anchored fluorescent silica NPs (FSNPs). Reprinted with permission from Jiao et al. [81]. Further permissions related to the material excerpted should be directed to the ACS

Nph) has been designed for guided photodynamic therapy to treat triple negative breast cancer (TNBC) [88]. After intravenous administration and selective accumulation inside the TNBC tissues, the nanoplatform undergoes a cathepsin-B cleavage restoring the prequenched NIR fluorescence and photodynamic activities of SQ and the Nph for magnetic resonance/near-infrared fluorescence (MR/NIRF) imaging. This nanoprobe showed a turn-on NIRF imaging response that sufficiently enhanced the single oxygen production, stability and targetability. With respect to squaraine incorporation in organic NPs, though literature is limited, few reports are found on albumin [20] and recently on powder chitosan system [89] which results in the enhancement of fluorescence quantum yield and lifetime, and high specificity, high stability and low dark toxicity.

4.2 Cyanine-based NPs

As already described for squaraine-based NPs, inorganic materials can be exploited to develop nanoplatforms for PDT. Silica NPs have also been used for the incorporation of cyanines to improve the shortcomings in physiological conditions such as the Aggregation Caused Quenching (ACQ). To this purpose, Jiao et al. [81] built hydrophobic structurally rigid silica nanoparticles loaded with a Cy7. As shown in Fig. 10, this cage can inhibit the ACQ effect providing a nonpolar microenvironment for the cyanine dye that can maintain its excellent photophysical properties both in water solution and in living cells due to the limitation of molecular motion. This nanosystem can provide long-term bright fluorescence imaging and a stable PDT process.

Another example is the incorporation of ICG in Au@SiO_2@mSiO_2 nanoplatforms to improve both photothermal and photodynamic activity [90]. The dense silica layer avoids the direct contact between the Au nanorod and ICG, also providing an optimal space between Au nanorods and ICG for an efficient plasmonic enhancement. In addition, ICG molecules are hosted and protected by the mesoporous silica layer allowing a higher singlet oxygen production under laser excitation compared to free ICG.

Another example to improve ICG application in PDT has been published by Gao et al. [91]. In this case, MnO_2 NPs were functionalized with hyaluronic acid and loaded with ICG. After laser irradiation, this nanosystem led to a significant tumor growth inhibition providing an alternative strategy to improve clinical PDT efficacy.

Among the different inorganic materials, Zhou et al. [92] reported multifunctional water stable nanoplatform based on iron oxide and a Cy7 (IR820) showing increased stability in water and an enhanced ability of singlet oxygen production compared to the free dye.

Biodegradable PEG–PCL (polyethylene glycol–polycaprolactone) polymeric NPs have played a great role in water solubility and fluorescence quantum yield enhancement of a hydrophobic cyanine derivative dye (IR775 dye). The encapsulation of IR775 in PEG-PCL NPs provides enhanced ROS generation and long circulation half lifetime in image-guided phototherapy compared to free ICG [93].

Hou et al. [94] provided a new approach to overcome tumor hypoxia and improve the IR820 PDT effect. They used hyaluronic acid modified poly(lactic-co-glycolic acid) (PLGA) nanoparticles loaded with IR820 and a catalase (CAT) which is able to catalyze H_2O_2 to produce oxygen in the cells. This process not only can regulate tumor hypoxia but can also provide oxygen to IR820 to enhance ROS production.

Thanks to their intrinsic excellent properties (*i.e.* water dispersibility/solubility, flexibility and biocompatibility) along with their ability to incorporate several active pharmaceutical agents, nanogels (NGs) have gained considerable attention as drug-delivery systems as alternative to polymeric NPs. Asadian et al. [95] used an optimized method of

incorporation of an indolenine-based Cy7 (IR806) in exogenous responsive nano-gel (tNG) to control stability and biocompatibility and enhance PDT efficacy of the system over the ovarian carcinoma cell line A2780.

More interestingly, multifunctionalized polymer-based NPs systems of poly (propargyl acrylate) (PA) were proposed as attractive "nanodevice" for personalized medicine [96]. PA NPs were functionalized with bovine serum albumin covalently conjugated to a Cy3. When administrated, these NPs exhibited an activation of emission due to the cleavage of the protein and release of the Cy fluorophore. Exploiting the digestion of protein, this smart "ON" and "OFF" nanoplatform system provided higher carcinoma cell death specifically on head and neck squamous cancer.

5 In vivo studies

Compared to the clinically approved PSs, such as porphyrins and their derivatives (i.e. Photofrin® and Foscan®), squaraine and cyanine dyes have been reported to potentially overcome the drawbacks related to the traditional PSs such as the poor light absorption, the low selectivity to the tumor cells and harmful photosensitivity on skin and eyes [44, 97]. In fact, by modifying the molecular structure, their core can be shaped and tailored to increase the chemo-physical features and exert different effects according to the desired application. Despite these promising premises, the steps to reach the effective use of SQ and CY molecules in the photodynamic treatment are still challenging. To date, to the best of our knowledge, no squaraines or cyanines have been approved or are commercially available for PDT treatment, as cyanines are currently only approved for imaging applications [98, 99]. The reason of this delay could be ascribed to a lack of in vivo studies reported in the literature, with a consequent poor information on the pharmacokinetic properties and preclinical evaluation, essential for a future spreading in the clinical trials. However, many encouraging in vitro studies, as reported in the previous sections, have demonstrated promising effectiveness of these dyes in PDT, providing the incentive for further in vivo investigations. The following paragraphs deal with a summary of the in vivo studies conducted over the recent years.

5.1 In vivo *PDT studies of squaraine dyes*

As far as squaraines are concerned, since Abraham et al. [100] reported the first in vivo experiments on phloroglucinol SQ **2c** as promising photosensitizers in PDT, only a limited number of works have reported the PDT potentiality of these PSs in vivo [43, 101, 102]. The bis(3,5-diiodo-2,4,6-trihydroxyphenyl) squaraine (**2c**) proved the ability to reduce the tumor size after PDT in the treatment of skin cancer in experimental mice models [100, 102], focusing the attention on the localization of the PS in the cellular environment. In this context, they proved that the dye accumulation does not occur in the nuclei, avoiding the DNA damage and genomic instability, but in the mitochondria, revealed by the presence of cytochrome C in the cytosol of the tumor area subjected to PDT. Since the cytochrome C release to the cytosol, due to the significant alteration of mitochondrial membrane permeability, is considered a crucial event in the mitochondria mediated pathway of apoptosis, they were able to confirm the crucial role of SQ in the induction of cell apoptosis [103, 104]. At the same time, the in vivo biodistribution of the dye on normal and skin tumor induced animal models has been investigated to evaluate the retention time of the dye [101]. After 24 h of injection, the dye has been clearly detected in the tumor site and in the immediate surroundings of the tumor, while no trace of SQ has been observed in the healthy tissues, confirming the selectivity of the dye for the tumor cells compared to the normal ones and the rapid clearance from the body. All this evidence highlighted as this squaraine can be evaluated as innovative photosensitizer for PDT, inducing reduction in the tumor volume with high selectivity and no cytotoxic effect for the healthy tissues.

The role of the SQ in in vivo PDT has also been reported by Wei et al. [43], who tested the PDT efficacy of a new dicyanomethylene substituted benzothiazole squaraine derivative (**2j**). After the dye intra-tumoral injection and once the tumor size reached 5–6 mm in diameter, the mice body weights, as well as the tumor sizes, were daily measured. Moreover, the histological sections of the tumors, liver, and kidney were analyzed after 14 days of treatments. The weight of all observed mice did not significantly change, demonstrating the non-toxicity of the dye. On the contrary, the analysis of tumor growth highlighted substantial differences in the different mice groups. In fact, the tumor volumes of all non-treated mice have grown over time, while in all 6 mice in the SQ + light group, tumor sizes were gradually reduced, confirming the excellent photodynamic behavior of the **2j** SQ in vivo. In addition, the analysis of histological sections revealed serious cellular damage in the groups treated with both SQ injection and laser irradiation compared to the controls, further supporting the safety and high efficacy of the squaraine in vivo.

5.2 In vivo *PDT studies of cyanine dyes*

Compared to squaraines, a greater number of studies are reported on the use of cyanines in in vivo PDT, because of their wider use as imaging probes and commercial availability. Modifications of ICG and other Near-infrared Fluorescence (NIRF) probes led to a large variety of structures employed in PDT studies. By modifying the chemical

structure of the commercially available IR-783 cyanine dye, Atchison and co-workers [61] were able to design a new class of sensitizers to be used in NIR activated photodynamic therapy. Specifically, two iodinated Cy7 (**6c** and **6d**) were synthesized and evaluated both in vitro and in vivo. The authors reported an enhanced PDT mediated cytotoxicity of the iodinated dye compared with the non-iodinated and clinically approved analogue (ICG), as well as a significantly reduction of tumor size after the PDT treatment of mice bearing ectopic human xenograft BxPC-3 pancreatic tumors. In addition, the mono-iodinated (**6c**) dye has further been proved to enable real-time NIR fluorescence imaging in vivo, confirming the ability of the sensitizer to selectively accumulate in the tumor site, avoiding damage to surrounding healthy tissue.

Despite the demonstrated photoactivity of the cyanine to treat and reduce tumors [61, 62, 105, 106], a single phototherapy approach seems to limit the in vivo therapeutic efficacy, particularly to treat extended and deep tumors [76, 107–109]. To overcome these drawbacks, a promising strategy could be the combination of different phototherapeutic approaches such as photodynamic and photothermal therapies. In fact, PDT depletes oxygen in tumor tissues leading to local hypoxia, and thus to low response to the therapy [11, 110], while PTT can cause an incomplete tumor destruction and thus tumor recurrence [76]. By combining these two phototherapeutic approaches, the local hyperthermia induced by PTT allows an increase in the intratumoral blood flow and oxygenation, promoting the ROS generation and thus the PDT activity. To this purpose, Cao et al. [62] demonstrated how the introduction of a synergistic photodynamic and photothermal treatments could further increase the therapeutic potential of the iodinated cyanines. The use of the indolenine-based Cy7 **6a** showed a significant delay in the tumor growth compared with commercial ICG derivatives (inhibition ratio 39.8 and 21.7%, respectively). In addition, as shown in Fig. 11, the reduction in the tumor growth is completed suppressed when the combination of PDT and PTT is applied (inhibition ratio 100%), confirming the feasibility of the synergistic approach to treat deep and large tumors.

To further increase the potential application of cyanines for in vivo treatments, their selective absorption by tumor cells as well as their fluorescent signals can be also exploited for diagnostic purpose, obtaining a single powerful platform which can simultaneously provide both cancer imaging and synergistic effect induced by PDT and PTT. As already reported in Sect. 2.2, Chi et al. [75] recently proposed a promising strategy demonstrating the in vivo synergistic phototherapy effects induced by a theragnostic nanocarrier consisting of hyaluronic acid (HA) and polyethylene glycol (PEG) incorporating an iodinated cyanine (HA-PEG-CyI, HPC). The proposed multi-functional nanoplatform is able to selectively accumulate in the tumor area and, by exploiting the optical imaging-guided NIR laser irradiation, the reduction of tumor volume can be selectively obtained thanks to the synergistic antitumor efficacy of both PDT and PTT. In addition, by tailoring the power density of the laser irradiation, the PDT/PTT efficacy can also be modulated. In fact, using high laser irradiation (0.96 W cm^{-2}) the designed system HPC showed both in vivo PDT/PTT efficacy, while using low laser irradiation (0.3 W cm^{-2}) only PDT efficacy can be exploited. The authors also observed the induction of a severe immune response, responsible of a secondary death of tumor cells and of the reduction of the tumor recurrence. Overall, all the results taken together confirmed the potential of this promising multifunctional approach for clinical applications.

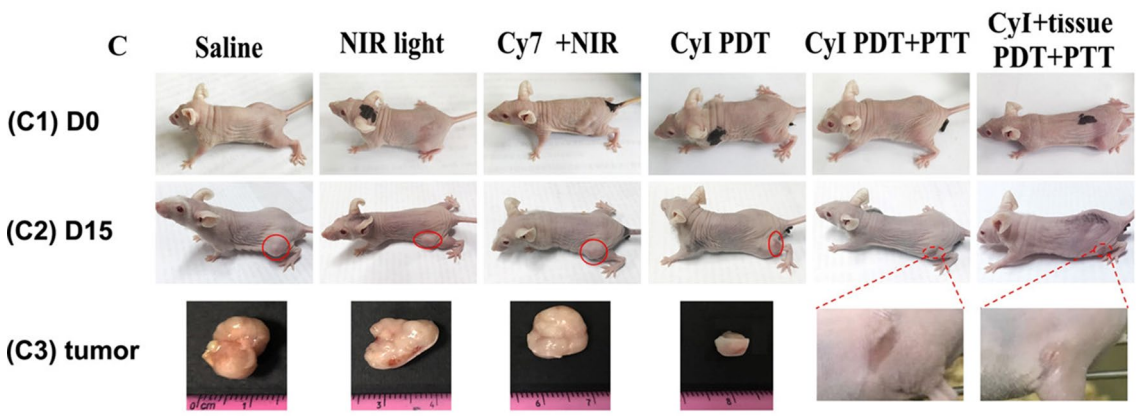

Fig. 11 Images of mice before treatment (C1) and after different treatments in day 15 (C2); (C3) tumor pictures after different treatments in day 15; enlarged pictures showed the heeled bar of tumors in CyI-treated mice (left) and CyI-treated tumors cover with 1 cm pork tissue (right) under NIR irradiation (808 nm, 0.96 W cm^{-2}, 1 min. Adapted with permission from Cao et al. [62]. Copyright 2019, American Chemical Society

By following these examples, to date, several works reporting different cyanines and nanosystems highlighted the in vivo efficacy of a synergistic PDT/PTT approach combined with imaging to increase the effectiveness of the treatment [76, 111–113]. Despite these promising results, one of the major unsolved concerns which hinders the clinical translation of PDT still remains the accumulation of PS in non-cancerous cells and therefore the low selectivity, which can lead to PS accumulation in healthy tissues and thus to serious side effects (such as prolonged skin photosensitivity). To increase the selectivity, different strategies have been proposed, spanning from the modification of the cyanine chemical structure [69, 114, 115], or the conjugation with polymeric nanocarriers [67, 116] to the supramolecular assemblies of organic monomers [71].

As mentioned before, PDT causes a depletion of oxygen in tumor tissues leading to local hypoxia, which can limit the therapy efficacy. Wang and co-workers [117] exploited this situation to design nanoparticles able to combine both photodynamic and hypoxia-activated therapies. Specifically, the PLGA/lipid nanoparticles containing both the indocyanine green as photosensitizer and the hypoxia-activated prodrug tirapazamine (TPZ) have been tested against metastatic breast cancer. In addition, to increase the selectivity for cancer cells, and thus improve the efficiency and limit the side effects, the nanoparticles were further conjugated with iRGD cyclic peptide, able to target them in solid tumors. Once internalized and irradiated with a NIR laser, the ICG incorporated into the NPs will produce ROS, causing the cell death and, in the meantime, the hypoxic condition, responsible of the TPZ activation, further increasing the cell death. The in vivo results demonstrated the selective tumor accumulation and intratumoral penetration of the nanoparticles, along with the total inhibition of the primary orthotopic tumor growth thanks to the synergistic effect of the PDT induced by the cyanine and the chemotherapeutic effect induced by the hypoxia activated TPZ. Moreover, since the orthotopic 4T1 model used in this study spontaneously tends to cause lung metastases, the authors investigated also the antimetastatic effect of the nanoparticles, confirming the efficacy of the designed system also against the lung metastatic lesions compared with the control groups.

6 Conclusions

Through the present review, despite the evident limits of squaraines and cyanines, we have shown their efficacy as alternative promising photosensitizers to treat cancer diseases. We have covered several topics ranging from a structure–activity analysis of the polymethine dyes described in literature as PDT photosensitizers to different approaches to overcome their limitations to boost their knowledge and the spreading of their use in PDT.

Compared to the first- and second-generation PSs, squaraine and cyanine dyes have been proved to show excellent photophysical and chemical properties such as broad absorption spectral range with high extinction coefficients, high fluorescence quantum yield and low dark toxicity and side effects. One of the most important features is the possibility of easily tuning their structure to obtain a strong absorption in the NIR region to match the biological tissues' transparency window as well as to increase the selectivity for the target tumor cells. In addition, thanks to the strong NIR absorption, PMDs can play different roles leading to a combination of different therapies such as synchronous and synergistic PDT/PTT effect and imaging-guided phototherapy, allowing to improve the elimination of the tumor and simultaneously monitor the progress of the PDT.

Nevertheless, a real structure–activity relationship study is still lacking in literature. In fact, very few papers reported a comprehensive evaluation of how the structural modifications of the compounds can affect the phototherapeutic effect. For instance, concerning cyanine and aminosquaraine dyes, studies on the effect of the different counterions and alterations of the central bridge are limited. In addition, for all PMDs, very few evaluations of the effect of the lateral chain modification have been published. There is a quite variety of structures for squaraines while the cyanines heterogeneity is still limited since only indolenine-based dyes are described. One main perspective for future assessment could be the employment of different heterocycles, already introduced for squaraines (i.e. benzothiazole, benzoselenazole, quinoline), in the synthesis of novel symmetric cyanines. All these possible modifications could lead to an improvement of the overall photophysical properties as well as the phototherapeutic potential.

So far, the spreading in the use and application of this class of dyes for PDT is still limited due to their poor chemical stability and solubility in biological environment and relatively low selectivity to tumor cells. In particular, the poor water solubility results in a low fluorescence intensity due to the self-quenching effect, leading to a reduction in the reactive oxygen species (ROS) generation. In this review, several examples have been reported to improve the solubility and avoid aggregation and, among them, self-assembly and nanoparticles incorporation have been shown as promising approaches.

Along with the improvements of chemical and structural modification strategies, more efforts need to be devoted to increase the targeting and selectivity. Both the self-assembly and the incorporation into nanoparticles of different nature allow to design a multifunctional nanoplatform that perfectly matches these requirements. In fact,

the possibility to modify or functionalize the NPs surface allows to exploit the external stimuli such as the pH and hypoxic tumor microenvironments, obtaining powerful tools to overcome the defects of the PDT application.

Finally, from these premises, it is evident that polymethine dyes represent promising and suitable alternative photosensitizers for PDT, enriching the current stock of the permanently used molecules. Certainly, more efforts need to be devoted in the field of PMDs, in particular commitments and investments for in vivo studies and in pre-clinical trials to evaluate the pharmacokinetics properties, and further essential parameters such as the optimal delivery methods, the irradiation source and the potency.

By following the trend of the last years reported in Fig. 1, the number of studies could be expected to further increase, allowing the scientific and clinical community to make more exhaustive conclusions about squaraines and cyanines and to clarify their real potential in the photodynamic therapy.

Acknowledgements The authors thank the financial support from the University of Torino (Ricerca Locale ex-60%, Linea A, Bando 2020 and 2021) and from the Fondazione Cassa di Risparmio di Torino (CRT), Italy (II tornata 2019 RF. 2019.2260).

Declarations

Conflict of interest The authors declare that they have no known competing financial interests or personal relationships that could have appeared to influence the work reported in this paper.

References

1. Abdel-Kader, M. H. (2014). History of photodynamic therapy. *Photodynamic Therapy: From Theory to Application*. https://doi.org/10.1007/978-3-642-39629-8_1
2. Abdel-kader, M. H. (2016). CHAPTER 1. The journey of PDT throughout history: PDT from pharos to present. In H. Kostron & T. Hasan (Eds.), *Photodynamic Medicine* (pp. 1–21). Cambridge, UK: The Royal Society of Chemistry. https://doi.org/10.1039/9781782626824-00001.
3. Choi, J., & Kim, S. Y. (2020). Photothermally enhanced photodynamic therapy based on glutathione-responsive pheophorbide a-conjugated gold nanorod formulations for cancer theranostic applications. *Journal of Industrial and Engineering Chemistry, 85*, 66–74. https://doi.org/10.1016/j.jiec.2020.01.018
4. Wu, J., Sha, J., Zhang, C., et al. (2020). Recent advances in theranostic agents based on natural products for photodynamic and sonodynamic therapy. *View, 1*, 20200090. https://doi.org/10.1002/viw.20200090
5. Pérez-Laguna, V., Gilaberte, Y., Millán-Lou, M. I., et al. (2019). A combination of photodynamic therapy and antimicrobial compounds to treat skin and mucosal infections: A systematic review. *Photochemical and Photobiological Sciences, 18*, 1020–1029. https://doi.org/10.1039/c8pp00534f
6. Lan, M., Zhao, S., Liu, W., et al. (2019). Photosensitizers for Photodynamic Therapy. *Advanced Healthcare Materials, 8*, 1900132. https://doi.org/10.1002/adhm.201900132
7. Li, L., & Huh, K. M. (2014). Polymeric nanocarrier systems for photodynamic therapy. *Biomaterials Research, 18*, 1–14. https://doi.org/10.1186/2055-7124-18-19
8. Ruan, Z., Zhao, Y., Yuan, P., et al. (2018). PEG conjugated BODIPY-Br_2 as macro-photosensitizer for efficient imaging-guided photodynamic therapy. *Journal of Materials Chemistry B, 6*, 753–762. https://doi.org/10.1039/c7tb02924a
9. Zou, J., Yin, Z., Wang, P., et al. (2018). Photosensitizer synergistic effects: D–A–D structured organic molecule with enhanced fluorescence and singlet oxygen quantum yield for photodynamic therapy. *Chemical Science, 9*, 2188–2194. https://doi.org/10.1039/c7sc04694d
10. Serpe, L., Ellena, S., Barbero, N., et al. (2016). Squaraines bearing halogenated moieties as anticancer photosensitizers: Synthesis, characterization and biological evaluation. *European Journal of Medicinal Chemistry, 113*, 187–197. https://doi.org/10.1016/j.ejmech.2016.02.035
11. Felsher, D. W. (2003). Cancer revoked: Oncogenes as therapeutic targets. *Nature Reviews Cancer, 3*, 375–380. https://doi.org/10.1038/nrc1070
12. Alejandro, V. C., Mónica, F. P., Xelha, A. P., et al. (2020). Brominated BODIPYs as potential photosensitizers for photodynamic therapy using a low irradiance excitation. *Polyhedron, 176*, 114207. https://doi.org/10.1016/j.poly.2019.114207
13. Xia, G., & Wang, H. (2017). Squaraine dyes: The hierarchical synthesis and its application in optical detection. *Journal of Photochemistry and Photobiology, C: Photochemistry Reviews, 31*, 84–113. https://doi.org/10.1016/j.jphotochemrev.2017.03.001
14. Magalhães, Á. F., Graça, V. C., Calhelha, R. C., et al. (2017). Aminosquaraines as potential photodynamic agents: Synthesis and evaluation of in vitro cytotoxicity. *Bioorganic and Medicinal Chemistry Letters, 27*, 4467–4470. https://doi.org/10.1016/j.bmcl.2017.08.004
15. Chen, G., Sasabe, H., Igarashi, T., et al. (2015). Squaraine dyes for organic photovoltaic cells. *Journal of Materials Chemistry A, 3*, 14517–14534. https://doi.org/10.1039/c5ta01879j
16. He, J., Jo, Y. J., Sun, X., et al. (2021). Squaraine dyes for photovoltaic and biomedical applications. *Advanced Functional Materials, 31*, 1–35. https://doi.org/10.1002/adfm.202008201
17. Saccone, D., Galliano, S., Barbero, N., et al. (2016). Polymethine dyes in hybrid photovoltaics: Structure–properties relationships. *European Journal of Organic Chemistry*. https://doi.org/10.1002/ejoc.201501598
18. Beverina, L., & Sassi, M. (2014). Twists and turns around a square: The many faces of Squaraine chemistry. *Synlett, 25*, 477–490. https://doi.org/10.1055/s-0033-1340482
19. Beverina, L., & Salice, P. (2010). Squaraine compounds: Tailored design and synthesis towards a variety of material science applications. *European Journal of Organic Chemistry*. https://doi.org/10.1002/ejoc.200901297
20. Štacková, L., Muchová, E., Russo, M., Slavíček, P., Štacko, P., & Klán, P. (2020). Deciphering the structure–property

relations in substituted heptamethine cyanines. *Journal of Organic Chemistry, 85*, 9776–9790. https://doi.org/10.1021/acs.joc.0c01104
21. Wang, S.-B., Chen, Z.-X., Gao, F., et al. (2020). Remodeling extracellular matrix based on functional covalent organic framework to enhance tumor photodynamic therapy. *Biomaterials, 234*, 119772. https://doi.org/10.1016/j.biomaterials.2020.119772
22. Chen, J., Xu, Y., Gao, Y., et al. (2018). Nanoscale organic-inorganic hybrid photosensitizers for highly effective photodynamic cancer therapy. *ACS Applied Materials and Interfaces, 10*, 248–255. https://doi.org/10.1021/acsami.7b15581
23. Zhao, X., Ma, H., Chen, J., et al. (2019). An epidermal growth factor receptor-targeted and endoplasmic reticulum-localized organic photosensitizer toward photodynamic anticancer therapy. *European Journal of Medicinal Chemistry, 182*, 111625. https://doi.org/10.1016/j.ejmech.2019.111625
24. Wang, Y., Li, Y., Yan, Q., et al. (2020). Benzocaine-incorporated smart 1,3-squaraine dyes: Red emission, excellent stability and cell bioimaging. *Dyes and Pigments, 173*, 1–7. https://doi.org/10.1016/j.dyepig.2019.107977
25. Sreejith, S., Carol, P., Chithra, P., & Ajayaghosh, A. (2008). Squaraine dyes: A mine of molecular materials. *Journal of Materials Chemistry, 18*, 264–274. https://doi.org/10.1039/b707734c
26. Khopkar, S., & Shankarling, G. (2019). Dyes and pigments synthesis, photophysical properties and applications of NIR absorbing unsymmetrical squaraines: A review. *Dyes and Pigments, 170*, 107645. https://doi.org/10.1016/j.dyepig.2019.107645
27. Saccone, D., Galliano, S., Barbero, N., et al. (2016). Polymethine dyes in hybrid photovoltaics: Structure–properties relationships. *European Journal of Organic Chemistry, 13*, 2244–2259. https://doi.org/10.1002/ejoc.201501598
28. Ilina, K., MacCuaig, W. M., Laramie, M., et al. (2020). Squaraine dyes: Molecular design for different applications and remaining challenges. *Bioconjugate Chemistry, 31*, 194–213. https://doi.org/10.1021/acs.bioconjchem.9b00482
29. Saccone, D., Galliano, S., Barbero, N., et al. (2016). Polymethine dyes in hybrid photovoltaics: structure–properties relationships. *European Journal of Organic Chemistry, 2016*, 2244–2259. https://doi.org/10.1002/ejoc.201501598
30. Yi, R., Das, P., Lin, F., et al. (2019). Fluorescence enhancement of small squaraine dye and its two-photon excited fluorescence in long-term near-infrared I&II bioimaging. *Optics Express, 27*, 12360. https://doi.org/10.1364/oe.27.012360
31. Yano, S., Hirohara, S., Obata, M., et al. (2011). Current states and future views in photodynamic therapy. *Journal of Photochemistry and Photobiology, C: Photochemistry Reviews, 12*, 46–67. https://doi.org/10.1016/j.jphotochemrev.2011.06.001
32. Avirah, R. R., Jayaram, D. T., Adarsh, N., & Ramaiah, D. (2012). Squaraine dyes in PDT: From basic design to in vivo demonstration. *Organic and Biomolecular Chemistry, 10*, 911–920. https://doi.org/10.1039/c1ob06588b
33. Dichiara, M., Prezzavento, O., Marrazzo, A., et al. (2017). Recent advances in drug discovery of phototherapeutic non-porphyrinic anticancer agents. *European Journal of Medicinal Chemistry, 142*, 459–485. https://doi.org/10.1016/j.ejmech.2017.08.070
34. D'Alessandro, S., & Priefer, R. (2020). Non-porphyrin dyes used as photosensitizers in photodynamic therapy. *Journal of Drug Delivery Science and Technology, 60*, 101979. https://doi.org/10.1016/j.jddst.2020.101979
35. Ramaiah, D., Eckert, I., Arun, K. T., et al. (2002). Squaraine dyes for photodynamic therapy: Study of their cytotoxicity and genotoxicity in bacteria and mammalian cells. *Photochemistry and Photobiology, 76*, 672. https://doi.org/10.1562/0031-8655(2002)076%3c0672:sdfpts%3e2.0.co;2
36. Ramaiah, D., Joy, A., Chandrasekhar, N., et al. (1997). Halogenated squaraine dyes as potential photochemotherapeutic agents. Synthesis and study of photophysical properties and quantum efficiencies of singlet oxygen generation. *Photochemistry and Photobiology, 65*, 783–790. https://doi.org/10.1111/j.1751-1097.1997.tb01925.x
37. Ramaiah, D., Eckert, I., Arun, K. T., et al. (2004). Squaraine dyes for photodynamic therapy: Mechanism of cytotoxicity and DNA damage induced by halogenated squaraine dyes plus light (> 600 nm). *Photochemistry and Photobiology, 79*, 99. https://doi.org/10.1562/0031-8655(2004)79%3c99:sdfptm%3e2.0.co;2
38. Antony-Babu, S., Stien, D., Eparvier, V., et al. (2017). Multiple Streptomyces species with distinct secondary metabolomes have identical 16S rRNA gene sequences. *Science and Reports, 7*, 1–8. https://doi.org/10.1038/s41598-017-11363-1
39. Rapozzi, V., Beverina, L., Salice, P., et al. (2010). Photooxidation and phototoxicity of π-extended squaraines. *Journal of Medicinal Chemistry, 53*, 2188–2196. https://doi.org/10.1021/jm901727j
40. Shafeekh, K. M., Soumya, M. S., Rahim, M. A., et al. (2014). Synthesis and characterization of near-infrared absorbing water soluble squaraines and study of their photodynamic effects in DLA live cells. *Photochemistry and Photobiology, 90*, 585–595. https://doi.org/10.1111/php.12236
41. Soumya, M. S., Devi, D. G., Shafeekh, K. M., et al. (2017). Photodiagnosis and photodynamic therapy photodynamic therapeutic efficacy of symmetrical diiodinated squaraine in in vivo skin cancer models. *Photodiagnosis and Photodynamic Therapy, 18*, 302–309. https://doi.org/10.1016/j.pdpdt.2017.03.009
42. Soumya, M. S., Shafeekh, K. M., Das, S., & Abraham, A. (2014). Symmetrical diiodinated squaraine as an efficient photosensitizer for PDT applications: Evidence from photodynamic and toxicological aspects. *Chemico-Biological Interactions, 222*, 44–49. https://doi.org/10.1016/j.cbi.2014.08.006
43. Wei, Y., Hu, X., Shen, L., et al. (2017). Dicyanomethylene substituted benzothiazole squaraines: The efficiency of photodynamic therapy in vitro and in vivo. *eBioMedicine, 23*, 25–33. https://doi.org/10.1016/j.ebiom.2017.08.010
44. Martins, T. D., Lima, E., Boto, R. E., et al. (2020). Red and near-infrared absorbing dicyanomethylene squaraine cyanine dyes: Photophysicochemical properties and anti-tumor photosensitizing effects. *Materials (Basel), 13*, 1–17. https://doi.org/10.3390/ma13092083
45. Fernandes, T. C. D., Lima, E., Boto, R. E., et al. (2020). In vitro phototherapeutic effects of indolenine-based mono- and dithiosquaraine cyanine dyes against Caco-2 and HepG2 human cancer cell lines. *Photodiagnosis and Photodynamic Therapy, 31*, 101844. https://doi.org/10.1016/j.pdpdt.2020.101844
46. Mandim, F., Graça, V. C., Calhelha, R. C., et al. (2019). Evaluation of new iodinated aminosquaraines as potential sensitizers for photodynamic therapy. *Molecules, 24*, 863. https://doi.org/10.3390/molecules24050863
47. Friães, S., Silva, A. M., Boto, R. E., et al. (2017). Synthesis, spectroscopic characterization and biological evaluation of unsymmetrical aminosquarylium cyanine dyes. *Bioorganic Med Chem, 25*, 3803–3814. https://doi.org/10.1016/j.bmc.2017.05.022
48. Friães, S., Lima, E., Boto, R. E., et al. (2019). Photophysicochemical properties and in vitro phototherapeutic effects of iodoquinoline- and benzothiazole-derived unsymmetrical squaraine cyanine dyes. *Applied Sciences, 9*, 5414. https://doi.org/10.3390/app9245414
49. Ferreira, D. P., Conceição, D. S., Ferreira, V. R. A., et al. (2013). Photochemical properties of squarylium cyanine dyes. *Photochemical and Photobiological Sciences, 12*, 1948–1959. https://doi.org/10.1039/c3pp50132a
50. Lima, E., Boto, R. E., Ferreira, D., et al. (2020). Quinoline- and benzoselenazole-derived unsymmetrical squaraine cyanine dyes: Design, synthesis, photophysicochemical features and

light-triggerable antiproliferative effects against breast cancer cell lines. *Materials (Basel), 13*, 1–24. https://doi.org/10.3390/ma13112646
51. Magalhães, Á. F., Graça, V. C., Calhelha, R. C., et al. (2019). Synthesis, photochemical and in vitro cytotoxic evaluation of benzoselenazole-based aminosquaraines. *Photochemical and Photobiological Sciences, 18*, 336–342. https://doi.org/10.1039/c8pp00201k
52. Lima, E., Silva, J. F., Santos, A. O., et al. (2020). Dyes and pigments photodynamic activity of indolenine-based aminosquaraine cyanine dyes: Synthesis and in vitro photobiological evaluation. *Dyes and Pigments, 174*, 108024. https://doi.org/10.1016/j.dyepig.2019.108024
53. Lima, E., Ferreira, O., Gomes, V. S. D., et al. (2019). Dyes and pigments synthesis and in vitro evaluation of the antitumoral phototherapeutic potential of squaraine cyanine dyes derived from indolenine. *Dyes and Pigments, 167*, 98–108. https://doi.org/10.1016/j.dyepig.2019.04.007
54. Ilina, K., & Henary, M. (2021). Frontispiece: Cyanine dyes containing quinoline moieties: History, synthesis, optical properties, and applications. *Chemistry A European Journal, 27*, 4248. https://doi.org/10.1002/chem.202181361
55. Bilici, K., Cetin, S., Aydındogan, E., et al. (2021). Recent advances in cyanine-based phototherapy agents. *Frontiers in Chemistry, 9*, 1–15. https://doi.org/10.3389/fchem.2021.707876
56. Li, L., Chen, Y., Chen, W., et al. (2019). Photodynamic therapy based on organic small molecular fluorescent dyes. *Chinese Chemical Letters, 30*, 1689–1703. https://doi.org/10.1016/j.cclet.2019.04.017
57. Lange, N., Szlasa, W., Saczko, J., & Chwiłkowska, A. (2021). Potential of cyanine derived dyes in photodynamic therapy. *Pharmaceutics, 13*, 1–17. https://doi.org/10.3390/pharmaceutics13060818
58. Chinna Ayya Swamy, P., Sivaraman, G., Priyanka, R. N., et al. (2020). Near infrared (NIR) absorbing dyes as promising photosensitizer for photo dynamic therapy. *Coordination Chemistry Reviews, 411*, 213233. https://doi.org/10.1016/j.ccr.2020.213233
59. Huang, H., Long, S., Li, M., et al. (2018). Bromo-pentamethine as mitochondria-targeted photosensitizers for cancer cell apoptosis with high efficiency. *Dyes and Pigments, 149*, 633–638. https://doi.org/10.1016/j.dyepig.2017.11.010
60. Ciubini, B., Visentin, S., Serpe, L., et al. (2019). Design and synthesis of symmetrical pentamethine cyanine dyes as NIR photosensitizers for PDT. *Dyes and Pigments, 160*, 806–813. https://doi.org/10.1016/j.dyepig.2018.09.009
61. Atchison, J., Kamila, S., Nesbitt, H., et al. (2017). Iodinated cyanine dyes: A new class of sensitisers for use in NIR activated photodynamic therapy (PDT). *Chemical Communications, 53*, 2009–2012. https://doi.org/10.1039/c6cc09624g
62. Cao, J., Chi, J., Xia, J., et al. (2019). Iodinated cyanine dyes for fast near-infrared-guided deep tissue synergistic phototherapy. *ACS Applied Materials and Interfaces, 11*, 25720–25729. https://doi.org/10.1021/acsami.9b07694
63. Chen, J., Tan, X., Luo, S., et al. (2018). Identification of a mitochondria-targeting fluorescent small molecule for dual phototherapy. *Journal of Innovative Optical Health Sciences, 11*, 1–8. https://doi.org/10.1142/S1793545818500165
64. Liu, H., Yin, J., Xing, E., et al. (2021). Halogenated cyanine dyes for synergistic photodynamic and photothermal therapy. *Dyes and Pigments, 190*, 109327. https://doi.org/10.1016/j.dyepig.2021.109327
65. Jiao, L., Song, F., Cui, J., & Peng, X. (2018). A near-infrared heptamethine aminocyanine dye with a long-lived excited triplet state for photodynamic therapy. *Chemical Communications, 54*, 9198–9201. https://doi.org/10.1039/c8cc04582h
66. Yang, X., Bai, J., & Qian, Y. (2020). The investigation of unique water-soluble heptamethine cyanine dye for use as NIR photosensitizer in photodynamic therapy of cancer cells. *Spectrochimica Acta, Part A: Molecular and Biomolecular Spectroscopy, 228*, 117702. https://doi.org/10.1016/j.saa.2019.117702
67. Thomas, A. P., Palanikumar, L., Jeena, M. T., et al. (2017). Cancer-mitochondria-targeted photodynamic therapy with supramolecular assembly of HA and a water soluble NIR cyanine dye. *Chemical Science, 8*, 8351–8356. https://doi.org/10.1039/c7sc03169f
68. Tan, X., Luo, S., Long, L., et al. (2017). Structure-guided design and synthesis of a mitochondria-targeting near-infrared fluorophore with multimodal therapeutic activities. *Advanced Materials, 29*, 1704196. https://doi.org/10.1002/adma.201704196
69. Luo, S., Tan, X., Fang, S., et al. (2016). Mitochondria-targeted small-molecule fluorophores for dual modal cancer phototherapy. *Advanced Functional Materials, 26*, 2826–2835. https://doi.org/10.1002/adfm.201600159
70. Wen, Z., Liu, F., Liu, G., et al. (2021). Assembly of multifunction dyes and heat shock protein 90 inhibitor coupled to bovine serum albumin in nanoparticles for multimodal photodynamic/photothermal/chemo-therapy. *Journal of Colloid and Interface Science, 590*, 290–300. https://doi.org/10.1016/j.jcis.2021.01.052
71. Li, M., Sun, W., Tian, R., et al. (2021). Smart J-aggregate of cyanine photosensitizer with the ability to target tumor and enhance photodynamic therapy efficacy. *Biomaterials, 269*, 120532. https://doi.org/10.1016/j.biomaterials.2020.120532
72. Jeong, C., Kim, J., & Kim, Y. C. (2020). Fluorescence color-changeable branched-form heptamethine cyanine dye as a redox-responsive multi-functional drug delivery system for enhanced cancer diagnosis and chemophototherapy. *Journal of Industrial and Engineering Chemistry, 87*, 187–197. https://doi.org/10.1016/j.jiec.2020.04.001
73. Yuan, A., Qiu, X., Tang, X., et al. (2015). Self-assembled PEG-IR-780-C13 micelle as a targeting, safe and highly-effective photothermal agent for in vivo imaging and cancer therapy. *Biomaterials, 51*, 184–193. https://doi.org/10.1016/j.biomaterials.2015.01.069
74. Yang, B., Gao, G., Liu, L., et al. (2017). IR-780 loaded folic acid modified chitosan nanoparticles (FASOC-IR780 NPs) as a targeting and theranostic agent for breast cancer therapy. *Journal of Biomaterials and Tissue Engineering, 7*, 605–613. https://doi.org/10.1166/jbt.2017.1620
75. Chi, J., Ma, Q., Shen, Z., et al. (2020). Targeted nanocarriers based on iodinated-cyanine dyes as immunomodulators for synergistic phototherapy. *Nanoscale, 12*, 11008–11025. https://doi.org/10.1039/c9nr10674j
76. Miao, W., Kim, H., Gujrati, V., et al. (2016). Photo-decomposable organic nanoparticles for combined tumor optical imaging and multiple phototherapies. *Theranostics, 6*, 2367–2379. https://doi.org/10.7150/thno.15829
77. Zhang, X., Jiang, D. W., Yang, G. L., et al. (2021). A single-wavelength NIR-triggered polymer for in situ generation of peroxynitrite (ONOO−) to enhance phototherapeutic efficacy. *Chinese Journal of Polymer Science (English Edition), 39*, 692–701. https://doi.org/10.1007/s10118-021-2540-0
78. Rui, L. L., Cao, H. L., Xue, Y. D., et al. (2016). Functional organic nanoparticles for photodynamic therapy. *Chinese Chemical Letters, 27*, 1412–1420. https://doi.org/10.1016/j.cclet.2016.07.011
79. Bechet, D., Couleaud, P., Frochot, C., et al. (2008). Nanoparticles as vehicles for delivery of photodynamic therapy agents. *Trends in Biotechnology, 26*, 612–621. https://doi.org/10.1016/j.tibtech.2008.07.007

80. Song, J., Qu, J., Swihart, M. T., & Prasad, P. N. (2016). Near-IR responsive nanostructures for nanobiophotonics: Emerging impacts on nanomedicine. *Nanomedicine Nanotechnology, Biology and Medicine, 12*, 771–788. https://doi.org/10.1016/j.nano.2015.11.009
81. Jiao, L., Liu, Y., Zhang, X., et al. (2020). Constructing a local hydrophobic cage in dye-doped fluorescent silica nanoparticles to enhance the photophysical properties. *ACS Central Science, 6*, 747–759. https://doi.org/10.1021/acscentsci.0c00071
82. Kamaly, N., Yameen, B., Wu, J., & Farokhzad, O. C. (2016). Degradable controlled-release polymers and polymeric nanoparticles: Mechanisms of controlling drug release. *Chemical Reviews, 116*, 2602–2663. https://doi.org/10.1021/acs.chemrev.5b00346
83. Bhattarai, P., & Dai, Z. (2017). Cyanine based nanoprobes for cancer theranostics. *Advanced Healthcare Materials, 6*, 1–23. https://doi.org/10.1002/adhm.201700262
84. Ma, X., Feng, H., Liang, C., et al. (2017). Mesoporous silica as micro/nano-carrier: From passive to active cargo delivery, a mini review. *Journal of Materials Science and Technology, 33*, 1067–1074. https://doi.org/10.1016/j.jmst.2017.06.007
85. Sreejith, S., Ma, X., & Zhao, Y. (2012). Graphene oxide wrapping on squaraine-loaded mesoporous silica nanoparticles for bioimaging. *Journal of the American Chemical Society, 134*, 17346–17349. https://doi.org/10.1021/ja305352d
86. Miletto, I., Fraccarollo, A., Barbero, N., et al. (2018). Mesoporous silica nanoparticles incorporating squaraine-based photosensitizers: A combined experimental and computational approach. *Dalton Transactions, 47*, 3038–3046. https://doi.org/10.1039/c7dt03735j
87. Bagchi, D., Halder, A., Debnath, S., et al. (2019). Exploration of interfacial dynamics in squaraine based nanohybrids for potential photodynamic action. *Journal of Photochemistry and Photobiology, A: Chemistry, 380*, 111842. https://doi.org/10.1016/j.jphotochem.2019.05.005
88. Wang, Y., Jiang, L., Zhang, Y., et al. (2020). Fibronectin-targeting and cathepsin B-activatable theranostic nanoprobe for MR/fluorescence imaging and enhanced photodynamic therapy for triple negative breast cancer. *ACS Applied Materials and Interfaces, 12*, 33564–33574. https://doi.org/10.1021/acsami.0c10397
89. Ferreira, D. P., Conceic, D. S., Fernandes, F., et al. (2016). Characterization of a squaraine/chitosan system for photodynamic therapy of cancer. *Journal of Physical Chemistry, 120*, 1212–1220. https://doi.org/10.1021/acs.jpcb.5b11604
90. Zhang, B., Wei, L., & Chu, Z. (2019). Development of indocyanine green loaded Au@Silica core shell nanoparticles for plasmonic enhanced light triggered therapy. *Journal of Photochemistry and Photobiology, A: Chemistry, 375*, 244–251. https://doi.org/10.1016/j.jphotochem.2019.02.028
91. Gao, S., Wang, G., Qin, Z., et al. (2017). Oxygen-generating hybrid nanoparticles to enhance fluorescent/photoacoustic/ultrasound imaging guided tumor photodynamic therapy. *Biomaterials, 112*, 324–335. https://doi.org/10.1016/j.biomaterials.2016.10.030
92. Zhou, H., Hou, X., Liu, Y., et al. (2016). Superstable magnetic nanoparticles in conjugation with near-infrared dye as a multimodal theranostic platform. *ACS Applied Materials and Interfaces, 8*, 4424–4433. https://doi.org/10.1021/acsami.5b11308
93. Duong, T., Li, X., Yang, B., et al. (2017). Phototheranostic nanoplatform based on a single cyanine dye for image-guided combinatorial phototherapy. *Nanomedicine Nanotechnology, Biology and Medicine, 13*, 955–963. https://doi.org/10.1016/j.nano.2016.11.005
94. Hou, X., Tao, Y., Li, X., et al. (2020). Cd44-targeting oxygen self-sufficient nanoparticles for enhanced photodynamic therapy against malignant melanoma. *International Journal of Nanomedicine, 15*, 10401–10416. https://doi.org/10.2147/IJN.S283515
95. Asadian-Birjand, M., Bergueiro, J., Wedepohl, S., & Calderón, M. (2016). Near infrared dye conjugated nanogels for combined photodynamic and photothermal therapies. *Macromolecular Bioscience, 16*, 1432–1441. https://doi.org/10.1002/mabi.201600117
96. Burdette, M. K., Jenkins, R., Bandera, Y. P., et al. (2020). Click-engineered, bioresponsive, and versatile particle–protein–dye system. *ACS Applied Bio materials, 2*, 3183–3193. https://doi.org/10.1021/acsabm.9b00025.Click-Engineered
97. O'Connor, A. E., Gallagher, W. M., & Byrne, A. T. (2009). Porphyrin and nonporphyrin photosensitizers in oncology: Preclinical and clinical advances in photodynamic therapy. *Photochemistry and Photobiology, 85*, 1053–1074.
98. Olubiyi, O. I., Lu, F.-K., Calligaris, D., et al. (2015). Advances in molecular imaging for surgery. *Image-guided neurosurgery* (pp. 407–439). Elsevier.
99. Eyal, S. (2020). Molecular imaging of membrane drug efflux transporters activity in cancer. *Drug efflux pumps in cancer resistance pathways: From molecular recognition and characterization to possible inhibition strategies in chemotherapy* (pp. 97–120). Elsevier.
100. Gayathri Devi, D., Cibin, T. R., Ramaiah, D., & Abraham, A. (2008). Bis(3,5-diiodo-2,4,6-trihydroxyphenyl)squaraine: A novel candidate in photodynamic therapy for skin cancer models in vivo. *Journal of Photochemistry and Photobiology, B: Biology, 92*, 153–159. https://doi.org/10.1016/j.jphotobiol.2008.06.002
101. Ms, S., & Abraham, A. (2013). Preclinical evaluation of symmetrical iiodinated squaraine dye on experimental animal models. *Journal of Glycobiology, s1*, 1–6. https://doi.org/10.4172/2168-958x.s1-003
102. Devi, D. G., Cibin, T. R., & Abraham, A. (2013). Bis(3,5-diiodo-2,4,6-trihydroxyphenyl) squaraine photodynamic therapy induces in vivo tumor ablation by triggering cytochrome *c* dependent mitochondria mediated apoptosis. *Photodiagnosis and Photodynamic Therapy, 10*, 510–517. https://doi.org/10.1016/j.pdpdt.2013.04.005
103. Kessel, D., & Luo, Y. (1999). Photodynamic therapy: A mitochondrial inducer of apoptosis. *Cell Death and Differentiation, 6*, 28–35. https://doi.org/10.1038/sj.cdd.4400446
104. Oleinick, N. L., Morris, R. L., & Belichenko, I. (2002). The role of apoptosis in response to photodynamic therapy: What, where, why, and how. *Photochemical and Photobiological Sciences, 1*, 1–21. https://doi.org/10.1039/b108586g
105. Broadwater, D., Bates, M., Jayaram, M., Young, M., He, J., Raithel, A. L., Hamann, T. W., Zhang, W., Borhan, B., Lunt, R. R., & Lunt, S. Y. (2019). Modulating cellular cytotoxicity and phototoxicity of fluorescent organic salts through counterion pairing. *Scientific Reports, 9*, 15288. https://doi.org/10.1038/s41598-019-51593-z
106. Yang, Q., Jin, H., Gao, Y., et al. (2019). Photostable iridium(III)–cyanine complex nanoparticles for photoacoustic imaging guided near-infrared photodynamic therapy in vivo. *ACS Applied Materials and Interfaces, 11*, 15417–15425. https://doi.org/10.1021/acsami.9b04098
107. Lv, R., Yang, P., He, F., et al. (2015). A yolk-like multifunctional platform for multimodal imaging and synergistic therapy triggered by a single near-infrared light. *ACS Nano, 9*, 1630–1647. https://doi.org/10.1021/nn5063613
108. Lv, R., Yang, P., He, F., et al. (2015). An imaging-guided platform for synergistic photodynamic/photothermal/chemo-therapy with pH/temperature-responsive drug release. *Biomaterials, 63*, 115–127. https://doi.org/10.1016/j.biomaterials.2015.05.016
109. Jang, B., Park, J., Tung, C., et al. (2011). Gold nanorod—Photosensitizer. *ACS Nano, 5*, 1086–1094.

110. Coutier, S., Mitra, S., Bezdetnaya, L. N., et al. (2001). Effects of fluence rate on cell survival and photobleaching in meta-tetra-(hydroxyphenyl)chlorin–photosensitized Colo 26 multicell tumor spheroids¶. *Photochemistry and Photobiology, 73*, 297. https://doi.org/10.1562/0031-8655(2001)073%3c0297:EOFROC%3e2.0.CO;2
111. Luo, S., Yang, Z., Tan, X., et al. (2016). Multifunctional photosensitizer grafted on polyethylene glycol and polyethylenimine dual-functionalized nanographene oxide for cancer-targeted near-infrared imaging and synergistic phototherapy. *ACS Applied Materials and Interfaces, 8*, 17176–17186. https://doi.org/10.1021/acsami.6b05383
112. Teng, C. W., Amirshaghaghi, A., Cho, S. S., et al. (2020). Combined fluorescence-guided surgery and photodynamic therapy for glioblastoma multiforme using cyanine and chlorin nanocluster. *Journal of Neuro-oncology, 149*, 243–252. https://doi.org/10.1007/s11060-020-03618-1
113. Li, H., Wang, P., Deng, Y., et al. (2017). Combination of active targeting, enzyme-triggered release and fluorescent dye into gold nanoclusters for endomicroscopy-guided photothermal/photodynamic therapy to pancreatic ductal adenocarcinoma. *Biomaterials, 139*, 30–38. https://doi.org/10.1016/j.biomaterials.2017.05.030
114. Noh, I., Lee, D. Y., Kim, H., et al. (2018). Enhanced photodynamic cancer treatment by mitochondria-targeting and brominated near-infrared fluorophores. *Advancement of Science, 5*, 1–11. https://doi.org/10.1002/advs.201700481
115. Choi, P. J., Park, T. I. H., Cooper, E., et al. (2020). Heptamethine cyanine dye mediated drug delivery: hype or hope. *Bioconjugate Chemistry, 31*, 1724–1739. https://doi.org/10.1021/acs.bioconjchem.0c00302
116. Zhu, Y. X., Jia, H. R., Gao, G., et al. (2020). Mitochondria-acting nanomicelles for destruction of cancer cells via excessive mitophagy/autophagy-driven lethal energy depletion and phototherapy. *Biomaterials, 232*, 119668. https://doi.org/10.1016/j.biomaterials.2019.119668
117. Wang, Y., Xie, Y., Li, J., et al. (2017). Tumor-penetrating nanoparticles for enhanced anticancer activity of combined photodynamic and hypoxia-activated therapy. *ACS Nano, 11*, 2227–2238. https://doi.org/10.1021/acsnano.6b08731